HHS Public Access

Author manuscript

Vis Neurosci. Author manuscript; available in PMC 2022 May 12.

Published in final edited form as:

Vis Neurosci. ; 38: E007. doi:10.1017/S0952523821000067.

Cerebellar projections to the macaque midbrain tegmentum: Possible near response connections

Martin O. Bohlen[1], **Paul D. Gamlin**[2], **Susan Warren**[3], **Paul J. May**[3,4,5]

[1]Department of Biomedical Engineering, Duke University, Durham, North Carolina

[2]Department of Ophthalmology and Visual Sciences, University of Alabama at Birmingham, Birmingham, Alabama

[3]Department of Neurobiology and Anatomical Sciences, University of Mississippi Medical Center, Jackson, Mississippi

[4]Department of Ophthalmology, University of Mississippi Medical Center, Jackson, Mississippi

[5]Department of Neurology, University of Mississippi Medical Center, Jackson, Mississippi

Abstract

Since most gaze shifts are to targets that lie at a different distance from the viewer than the current target, gaze changes commonly require a change in the angle between the eyes. As part of this response, lens curvature must also be adjusted with respect to target distance by the ciliary muscle. It has been suggested that projections by the cerebellar fastigial and posterior interposed nuclei to the supraoculomotor area (SOA), which lies immediately dorsal to the oculomotor nucleus and contains near response neurons, support this behavior. However, the SOA also contains motoneurons that supply multiply innervated muscle fibers (MIFs) and the dendrites of levator palpebrae superioris motoneurons. To better determine the targets of the fastigial nucleus in the SOA, we placed an anterograde tracer into this cerebellar nucleus in *Macaca fascicularis* monkeys and a retrograde tracer into their contralateral medial rectus, superior rectus, and levator palpebrae muscles. We only observed close associations between anterogradely labeled boutons and the dendrites of medial rectus MIF and levator palpebrae motoneurons. However, relatively few of these associations were present, suggesting these are not the main cerebellar targets. In contrast, labeled boutons in SOA, and in the adjacent central mesencephalic reticular formation (cMRF), densely innervated a subpopulation of neurons. Based on their location, these cells may represent premotor near response neurons that supply medial rectus and preganglionic Edinger–Westphal motoneurons. We also identified lens accommodation-related cerebellar afferent neurons via retrograde trans-synaptic transport of the N2c rabies virus from the ciliary muscle. They were found bilaterally in the fastigial and posterior interposed nuclei, in a distribution which mirrored that of neurons retrogradely labeled from the SOA and cMRF. Our results suggest these cerebellar neurons coordinate elements of the near response during symmetric vergence and disjunctive saccades by targeting cMRF and SOA premotor neurons.

[*]**Corresponding author:** Paul J. May, pmay@umc.edu.

Author Contributions. The experiments were designed by P.J.M. and P.D.G., and were carried out by M.O.B., S.W., and P.J.M. Data analysis was done by M.O.B. and P.J.M. The manuscript was written by P.J.M. and edited by all authors.

Conflict of Interest. None of the authors has any conflicts of interest with respect to the findings of this study.

Keywords

vergence; oculomotor; saccade; fastigial; trans-synaptic transport

Introduction

Goal directed behaviors can be modified, based on practice and feedback, to more accurately accomplish their aim. An example of this plasticity is saccade adaptation, where systematically changing the target location while the saccade is being made results in a gradual change in saccade amplitude to acquire the shifted target (Hopp & Fuchs, 2004; Takeichi et al., 2007; Iwamoto & Kaku, 2010). The role of the cerebellum in this plasticity has been amply demonstrated (Barash et al., 1999; Soetedjo et al., 2008, 2019; Kojima et al., 2011). For smooth pursuit movements, which must track the speed and direction of the target, the cerebellum is again an important contributor to the behavior (Takagi et al., 2000; Lisberger, 2010; Dash & Thier, 2014; Raghavan & Lisberger, 2017; Bourrelly et al., 2018; Kim et al., 2019). In addition to saccades and smooth pursuit, a third form of volitional eye movement takes place: vergence. Vergence eye movements are made when the new target is located at a different distance from the viewer than the current one. They can accompany both saccades and smooth pursuit eye movements. In addition, for targets located on the visual midplane, eye movements just change the vergence angle. Vergence changes are accompanied by changes in the focal distance of the lens produced by the actions of the ciliary muscle, as well as by changes in pupil diameter. This combination of extraocular and intraocular changes is commonly referred to as the near triad. Consideration of the eye movements required by the complex three-dimensional world in which we live brings one to the conclusion that most eye behaviors involve this triad. Since the cerebellum is involved in modulating other types of eye movements, it would seem reasonable to propose that the cerebellum plays a role in coordinating these near triad functions, as well.

Estimating target distance requires a complex analysis of a variety of cues, including visual disparity, vergence angle, blur, ocular accommodation, target size, and perspective (Leigh & Zee, 2015; McCann et al., 2018). The capabilities of the cerebellum would seem well suited to ensuring precision in such a task. In fact, vergence is capable of adaptation (Schor & McCandless, 1995; Chaturvedi & van Gisbergen, 1997; Schor et al., 2002). For example, the cross coupling between the drive for lens accommodation and changes in vergence angle is plastic, and can be modified through the use of lenses (Maxwell & Schor, 1994). Furthermore, the human cerebellum displays activity related to changes in both vergence angle and lens accommodation (Richter et al., 2000, 2004; Takagi et al., 2003; Lv et al., 2020). In addition, cerebellar lesions produce losses in the ability to adapt aspects of the near response in humans (Milder & Reinecke, 1983; Sander et al., 2009; Leigh & Zee, 2015), and more recently, inactivation of the cerebellum using transcranial magnetic stimulation has been shown to affect the capacity for vergence adaptation (Erkelens et al., 2020).

Awake behaving monkey recording studies have established that vergence signals are present in the cerebellum. Cells encoding convergence pursuit signals have been observed in the vermis (Nitta et al., 2008), and cells firing during symmetric convergence have been

recorded in the fastigial nucleus (FN) (Zhang & Gamlin, 1996). In addition, cells firing during divergence have been recorded in the posterior interposed nucleus (PIN) (Zhang & Gamlin, 1998), where microstimulation produces divergence and accommodation for far targets. Inactivation of these cerebellar nuclei in monkeys with experimental strabismus leads to changes in vergence angle, with loss of the caudal FN producing divergence and loss of the PIN producing convergence (Joshi & Das, 2013). In anesthetized cats, electrical stimulation of these nuclei produces changes in lens accommodation (Hosoba et al., 1978) and cells in the PIN fire with respect to lens accommodation (Bando et al., 1979). One of the targets of these cerebellar nuclei is the supraoculomotor area (SOA) (May et al., 1992). This study suggested that the FN and PIN might target near response neurons located in this region. Near response neurons are premotor neurons whose tonic activity correlates with vergence angle and the degree of lens accommodation (cat: Bando et al., 1984; monkey: Mays, 1984; Judge & Cumming, 1986; Zhang et al., 1992). Furthermore, the firing of these neurons correlates with the inappropriate vergence angle observed in experimental strabismus (Das, 2012; Walton et al., 2019).

While there is good evidence that near response neurons are located within the SOA (Das, 2012; May et al., 2018b), the somata and/or dendrites of a variety of other cell types can be found within this area. Specifically, the peptidergic neurons of the centrally projecting Edinger–Westphal nucleus (EWcp) are located there in monkeys (May et al., 2008; Horn et al., 2008; Kozicz et al., 2011), and the dendrites of the preganglionic Edinger–Westphal (EWpg) motoneurons extend into the SOA (May et al., 2018b). Dendrites from levator palpebrae superioris (henceforth the levator) motoneurons located in the caudal central subdivision (CC) of the oculomotor nucleus (III) are also found in SOA (May et al., 2012). The other population of neurons present in the SOA is the C-group. The C-group contains motoneurons that supply multiply innervated muscle fibers (MIFs) in the medial and inferior rectus muscles (Büttner-Ennever et al., 2001), and their dendrites arborize within the SOA (Erichsen et al., 2014; Tang et al., 2015). In the extraocular muscles, MIFs are innervated by axons that make small boutonal contacts all along the length of the fiber, and which produce graded, as opposed to all-or-none, contractions (see Spencer & Porter, 2006 for review). It has been suggested that medial rectus MIFs play a special role in vergence eye movements (Erichsen et al., 2014; Bohlen et al., 2017a), although MIF motoneurons fire during all types of eye movement (Hernández et al., 2019). Other populations of MIF motoneurons, those of the superior rectus and inferior oblique muscles, lie in the S-group, which lies between the two sides of the oculomotor nucleus (Büttner-Ennever et al., 2001). These are also possible targets of the cerebellar input. Furthermore, based on data from the cat, it has been suggested that the dendrites of superior rectus motoneurons supplying singly innervated muscle fibers (SIFs) extend into the SOA (Edwards & Henkel, 1978).

In view of the many possible targets of the cerebellar nuclear projection to the SOA, we elected to use neuroanatomical means to investigate those targets listed above that are associated with eye movements. Consequently, we began this study by using dual tracer experiments in macaque monkeys to determine whether projections from the FN contact motoneurons supplying the medial rectus, superior rectus, or levator muscles. In addition, we identified the cells in the cerebellar nuclei that help control lens accommodation and

those which project to the cMRF by use of retrograde tracers to further our understanding of cerebellar nuclear control of the near response.

Materials and methods

Seven young adult *Macaca fascicularis* monkeys of both sexes (2.65–5.36 kg) were used in this study. All procedures were approved by the Institutional Animal Care and Use Committees of the University of Mississippi Medical Center or of the University of Pittsburgh, depending on where the surgeries occurred. They were done in accordance with the principles for care and use of animals adopted by the Society for Neuroscience. Animals were first sedated with ketamine HCl (10 mg/kg, IM), then intubated so that they could be anesthetized throughout surgery with isoflurane (1–3%). They were also given atropine sulfate (0.05 mg/kg, IM) to decrease airway secretions. The analgesic, Carprofen (3 mg/kg, IM), was given preemptively. In order to avoid edema, animals were treated with dexamethasone (2.5 mg/kg, IV). After closing, Marcaine was infused into the incision area. Following surgery, Buprenex (0.01 mg/kg, IM) was administered as an analgesic.

Dual tracer experiments

For dual tracer experiments that labeled cerebellar afferents and extraocular motoneurons, three animals underwent two surgical procedures with their heads placed in a stereotaxic apparatus (Koff Instruments, Tajunga, CA). In the first procedure, a midline incision was made in the scalp. A craniotomy was made above the target and the dura was reflected. Part of the medial bank of parietal and occipital cortex was then aspirated to reveal the tentorium cerebelli, which was cut and reflected to reveal the surface of the midline cerebellum. A 1.0 μl Hamilton syringe mounted in a micromanipulator (Kopf Instruments, Tajunga, CA) was used to inject 10% biotinylated dextran amine (BDA) (Molecular Probes/Thermo Fisher, Waltham, MA) into the left FN, which was located by the use of stereotaxic coordinates (Szabo & Cowan, 1984; Paxinos et al., 2000) adjusted with respect to the cerebellar surface. Each injection consisted of 0.1 μl of tracer. Three injections were made 0.3 mm apart along each track, and up to four tracks were made at rostrocaudal sites located 0.5 mm apart. The aspiration defect was filled with gelfoam and the scalp was reapproximated and stabilized with suture.

Nineteen days were allowed for transport of the BDA before the eye muscles were injected. Since previous studies have shown that the cerebellar nuclear input to the SOA is denser on the contralateral side (May et al., 1992), the right orbit contralateral to the FN injection was approached by making an incision along the brow. The orbicularis oculi muscle was disinserted from its attachment to the superior orbital ridge. The levator muscle, superior rectus muscle, and the medial rectus muscle were each isolated and injected with a mixture of 1% cholera toxin subunit B conjugated to horseradish peroxidase (ChTB-HRP) and 1% wheat germ agglutinin conjugated horseradish peroxidase (WGA-HRP) (Sigma-Aldrich, St. Louis, MO). This mixture was used in an attempt to maximize dendritic labeling, although it also increased spread to other muscles. The levator was injected with 5.0 μl and the rectus muscles with 7.0 μl by use of a 10 μl Hamilton syringe. The orbicularis oculi muscle was also injected with the tracers (5 μl), as it is an antagonist of the levator muscle during

blinks. It was then reattached to its insertion and the incision was closed by means of suture. After two additional days of survival for tracer transport, the animals were again sedated with ketamine HCL (10 mg/kg, IM) and then deeply anesthetized with sodium pentobarbital (50 mg/kg, IP). They were subsequently perfused through the heart with a 0.1 M, pH 7.2 phosphate buffered saline rinse, followed by a fixative containing 1.0% paraformaldehyde and 1.5% glutaraldehyde in 0.1 M, pH 7.2 phosphate buffer (PB). The brains were blocked in the frontal plane and post-fixed in the same fixative solution, before being stored in 0.1 M, pH 7.2 PB at 4°C.

A vibratome (Leica VT100S, Buffalo Grove, IL) was used to cut the brains at 100 μm, and sections were collected in 0.1 M, pH 7.2 PB. At a minimum, a one in three series of sections was processed to reveal both tracers. First, the sections were reacted to reveal the HRP. They were placed in a solution that contained 0.25% ammonium molybdate in 0.1 M, pH 6.0 PB, followed by incubation overnight at 4°C in a solution that contained 0.5% tetramethylbenzidine (TMB) and 2.5% ethanol in the same ammonium molybdate PB solution with 0.00375% H_2O_2. The resultant blue reaction product was then stabilized in 5.0% ammonium molybdate in 0.1 M, pH 6.0 PB. Next, it was protected by reacting the sections in a solution containing 0.5% diaminobenzidine (DAB) in 0.1 M, pH 7.2 PB with 0.005% H_2O_2 to produce a brown reaction product. To reveal the location of the BDA, the sections were subsequently incubated overnight at 4°C in a 0.2% avidin-HRP solution containing 0.3% Triton X-100 in 0.1 M, pH 7.2 PB. They were then rinsed and reacted in a solution containing 0.5% DAB in 0.1 M, pH 7.2 PB with 0.005% H_2O_2. This solution also contained 0.1% nickel ammonium sulfate and 0.05% cobalt chloride so that it produced a black reaction product in the labeled axons. After rinsing, the sections were mounted on gelatin coated slides, counterstained with cresyl violet, dehydrated, cleared, and coverslipped.

Rabies experiments

To identify the cells in the cerebellum supplying input to the premotor neurons that control the lens accommodation component of the near response, we used retrograde trans-synaptic transport of rabies virus. The surgical procedures were carried out at the Systems Neuroscience Institute with the support of the Center for Neuroanatomy with Neurotropic Viruses, located at the University of Pittsburgh Medical Center. For this study, the ciliary muscles of the left eye of two *M. fascicularis* monkeys were injected with the N2c strain of rabies virus. The cornea was first desensitized with ophthalmic Proparacaine (0.5%) drops. A 25G needle attached to a 100 μl Hamilton syringe was inserted into the ciliary body at ~12 sites around the perimeter of the iris, and a total of 150 μl of solution containing 5×10^9 plaque forming units/ml was injected. Our previous studies indicated that motoneurons in the EWpg are labeled at 66 h after injection, and premotor neurons supplying these motoneurons are labeled between 72 and 76 h after the injection (May et al., 2018b; 2019). Therefore, we used a survival time of 84 h to label the cerebellar cells supplying these premotor neurons. At this point in time, the animals were perfused with 0.1 M, pH 7.2 phosphate buffered saline rinse, followed by a fixative containing 4.0% paraformaldehyde in 0.1 M, pH 7.2 PB. This fixative was followed by a second fixative mixture that also

contained 5% glycerol. The brains were blocked in the frontal plane and post-fixed in a 4.0% paraformaldehyde 0.1 M, pH 7.2 PB solution containing 10% glycerol as a cryoprotectant.

The brains were frozen and sectioned at 50 μm on a sliding microtome (American Optical). A minimum of one in five sections was processed to reveal the location of the neurons infected with the rabies virus. Sections were placed in 0.3% H_2O_2 to decrease background peroxidase levels. Blocking was produced by incubation in 1.5% normal horse serum with 0.3% Triton X-100 in a 0.1 M, pH 7.4 combination of phosphate and Trizma buffer with 0.05% sodium azide (PTA). The primary antibody, a mouse monoclonal against the rabies virus, was diluted 1:1000 in PTA. (The antibody, designated 31G10, was a gracious gift of Matthias Schnell of Thomas Jefferson University, Philadelphia, PA.) This antibody has been previously characterized and shown to be highly specific and effective (Raux et al., 1997; Ruigrok et al., 2016). In control sections, we eliminated the primary or secondary antibody steps and found no labeling. The incubation lasted for 2 days with agitation at 4°C. The antibody was tagged with biotin labeled secondary antibody, and then avidin-HRP, through the use of the appropriate ABC Kit (Vector Labs, Burlingame, CA). To visualize the labeled cells, sections were reacted in DAB as described above for the brown reaction product, before being mounted, in some cases counterstained, then dehydrated, cleared and coverslipped.

cMRF injection experiments

In order to compare the results from the rabies experiments to conventional labeling of cerebellar afferents to the cMRF, we injected this region with 2% WGA-HRP in 2 *M. fascicularis* monkeys. We utilized the same approach as described for the cerebellar injections, but aspirated cortex further rostrally, so that the surface of the superior colliculus and the caudal pole of the pulvinar could be visualized. A 1.0 μl Hamilton syringe was angled 15° tip rostral in the sagittal plane, and then rotated 10°, moving the tip toward the midline, before advancing it through the pulvinar toward the coordinates of the cMRF. There, a single 0.05 μl injection of tracer was made. The animals survived for 2 days and were then perfused. Their brains were cut as described for the dual tracer experiments, except that only 1.25% glutaraldehyde was used in the fixative. They were then processed to reveal the blue TMB reaction product as described above.

Analysis

Chartings and high magnification drawings were made using an Olympus BH-2 microscope (Olympus, Center Valley, PA) equipped with a drawing tube. Low magnification section drawings were made with a Wild M8 stereoscope (Leica Microsystems, Buffalo Grove, IL) with attached drawing tube. Photomicrographs were made with a Nikon Eclipse E600 microscope using a Nikon DS-Ri1 digital camera controlled by Nikon Elements software (Nikon Instruments, Inc., Melville, NY). Multiple *Z*-axis focal planes were combined digitally. The brightness and contrast of the images were adjusted to match the view seen by the eye through the use of Adobe Photoshop (Adobe, San Jose, CA).

Results

Dual tracer experiments

The results from a dual tracer case are shown in Fig. 1. In this example, the injection spread from the left FN to include a portion of the two left interposed nuclei (Fig. 1G–1I). The distribution of terminal label (red stipple) within the SOA is bilateral, but is somewhat denser contralateral to the injection site (Fig. 1A–1F). Labeled terminal arbors in the SOA are more common caudally (Fig. 1F). The pattern of retrogradely labeled motoneurons (blue diamonds) was, for the most part, confined to the superior rectus pool on the left (Fig. 1C–1F), the medial rectus pools on the right (Fig. 1A–1F) and the levator pool in the caudal central subdivision (CC) of oculomotor nucleus (III) (Fig. 1F). There was some evidence of spread of the retrograde tracer to other extraocular muscles supplied by motoneurons in the rostral end of the right III (Fig. 1A and 1B). As a consequence, it is possible that the labeled C-group population may include inferior rectus MIF motoneurons, as well as medial rectus MIF motoneurons. There was overlap between the distributions of labeled terminals and labeled cells in the area of the C-group and in the CC. However, the distribution of labeled terminals did not overlap with superior rectus motoneurons within III (Fig. 1C–1F) or with the S-group motoneurons, which are MIF motoneurons that are located between the two sides of III (Fig. 1B–1E).

The higher magnification illustration from this case (Fig. 2) gives a more detailed view of the overlap with MIF motoneurons in C-group. There is overlap between the labeled terminal arbors (red) and some, but not all, of the labeled C-group cells (shading). Most of the close associations (green arrowheads) between labeled boutons and labeled motoneurons were found on dendrites that extend into the SOA, and not on motoneuron somata. In fact, the terminal field is considerably denser in the SOA above the C-group. There, examples where labeled boutons outlined individual counterstained neurons (short green arrow) are present. Similar examples containing C-group motoneurons with dendrites extending into the SOA are shown in Fig. 3A and 3D. In a number of cases, close associations (arrowheads) could be observed between the black, BDA labeled axonal boutons and the brown, HRP labeled dendrites (Fig. 3C). Close associations with more proximal dendrites and somata, like those shown in Fig. 3E–3F, were rarer. Within the SOA, we sometimes observed dense collections of labeled boutons. As shown in Fig. 3B, labeled boutons clustered around counter-stained somata (arrow) were present. These boutons radiated out from the soma, and appeared to outline its dendrites.

Fig. 4 illustrates the relationship of the labeled cerebellar terminal arbors (red) with the labeled levator motoneurons (shaded) in this same case. While some labeled terminal arbors were actually found within the borders of the CC, most of the overlap between labeled elements occurred in the SOA. There, the dendrites of those levator motoneurons located dorsally within CC extended into the SOA terminal field and formed close associations (arrowheads) with labeled boutons found there. Note that most of the levator motoneurons did not display close associations with cerebellar boutons. The characteristics of the levator population are further demonstrated in Fig. 5. The extensive bilateral retrograde labeling of levator motoneurons from an injection on one side is shown in the lower magnification

views (Fig. 5A and 5E). Higher magnification views (Fig. 5B, 5D, and 5F) show close associations (arrowheads) between labeled boutons and labeled distal dendrites. Close associations between labeled boutons and proximal dendrites (Fig. 5C) were relatively rare. Labeled cerebellar terminals were not observed either in close association with retrogradely labeled orbicularis oculi motoneurons located in the dorsal subdivision of the right facial nucleus, or in the dorsal subdivision of the left facial nucleus. Consequently, we will not discuss this point further.

A similar pattern of terminal labeling was observed when only the FN was injected. Fig. 6 shows the distribution of anterogradely labeled terminal arbors (red) and retrogradely labeled motoneurons (blue diamonds) from a dual tracer case in which the BDA injection site did not invade the interposed nuclei (Fig. 6E–6G). The labeled terminals were again present bilaterally in the SOA with a distinct contralateral predominance (Fig. 6A–6D), and were denser caudally. Compared to the terminal fields observed in the previous case (Fig. 1) these were denser just above III. This matches the findings from anterograde transport of WGA-HRP, where the FN terminal field in the SOA was more ventrally located than the PIN terminal field (May et al., 1992). In this case, the widespread distribution of retrograde label indicated that the tracer spread outside the injected muscles, particularly into the inferior rectus muscle, and to a lesser extent into the inferior oblique muscle (Fig. 6A–6D). No overlap with labeled fastigial terminals was observed for the superior rectus motoneurons in the left III, or in the S-group, between the nuclei (not shown). The set of motoneurons located dorsal to the right nucleus represents the C-group. There was overlap between labeled cells and labeled terminals in this region. Levator motoneurons were also labeled in CC (Fig. 6D), and showed some overlap with labeled terminals. Closer examination (not illustrated) revealed that there were nearly as many close associations between labeled terminals and levator motoneuron dendrites in SOA as in the previous case (Fig. 4). The area of SOA within the green box in Fig. 6C is illustrated at higher magnification in Fig. 6H. The BDA labeled axons produced numerous terminal arbors characterized by *en passant* boutons. The retrogradely labeled C-group motoneurons (shaded) displayed labeled dendrites extending well out into SOA. A number of close associations (arrowheads) were present between the labeled dendrites and labeled terminal arbors.

Further examples of close associations observed between the labeled boutons and MIF motoneurons in this case are shown in Fig. 7. The brown, labeled C-group motoneurons sit ventral to numerous black labeled terminal arbors in SOA (Fig. 7A and 7C). The higher magnification view of one of these MIF motoneurons (Fig. 7B) reveals the presence of several close associations (arrowheads) with labeled boutons. Other examples were present in this case (Fig. 7E and 7F), but the majority of C-group cells did not display close associations. Within the SOA, we sometimes observed a striking collection of labeled boutons. As shown in Fig. 7C and 7D, the labeled boutons appeared to cluster around a counterstained soma (arrow) and could be observed radiating out from the soma, apparently outlining its primary and secondary dendrites.

Our previous anatomical work (May et al., 2019) and physiological studies (Mays et al., 1986) have suggested that a second population of near response neurons is present in the cMRF. Consequently, we examined this region as well. In the illustrated case, the injection

site includes the caudal pole of the FN on the right, and adjacent portions of the left FN (Fig. 8F and 8G). As with the other two cases, bilateral terminal labeling (red stipple) was present in the SOA (Fig. 8A–8E), but it was considerably sparser, presumably due to the smaller area of FN injected. The bilateral terminal distribution in SOA did not show a side preference since both FN were involved in the injection site. In this case, just the superior rectus, medial rectus and levator motor pools were retrogradely labeled (blue diamonds) (Fig. 8A–8E). In the case of both the C-group and the levator motoneurons there was overlap between the distribution of labeled terminals and cells. However, the number of C-group cells that showed close associations, like the one shown in Fig. 9E and 9G, was quite small. The same finding applied to the levator motoneurons, where fewer close associations were encountered (not illustrated). Within SOA, examples of highly innervated cells (Fig. 9E and 9F) were still present, despite the much sparser terminal field.

Labeled terminal arbors were present throughout the cMRF (Fig. 8B–8E) on both sides of the brainstem. However, the labeling on the left, contralateral to the bulk of the injection, was both heavier and more widespread. Examination of the cMRF in the other two cases (whose injection sites are shown in Figs. 1 and 6) showed a similar level of cMRF terminal labeling, but an even stronger contralateral preference. As in the SOA, the propensity for the bouton labeling to pick out and intensively innervate a subset of neurons was observed in the cMRF in this and the other cases. The large number of boutons contacting these cMRF neurons can be appreciated in Fig. 9A–9D. Most of these were present in the left cMRF (Fig. 9A–9C), contralateral to the main area of the FN injection, but occasional examples (Fig. 9D) were also present in the right cMRF. The cerebellar boutons in the cMRF not only picked out the somata of specific neurons, they also appeared to follow the contours of their dendritic field. Two examples (arrows) of this characteristic are illustrated in Fig. 10. Note that in the area around these cells, there are also labeled axons that do not show this arrangement.

Rabies experiments

In view of the close relationship of lens accommodation and vergence, we next examined the location of the neurons in the cerebellar nuclei that are connected to the ciliary muscle. The distribution of cells (red dots) within the deep cerebellar nuclei that were trans-synaptically labeled at 84 h following injections of rabies into the ciliary muscle of the left eye is shown in Fig. 11. The vast majority of trans-synaptically labeled neurons were present in the caudal portion of the FN (Fig. 11A–11E) and in the ventrolateral portion of the PIN (Fig. 11A–11F). A few cells were observed in the anterior interposed nucleus (Fig. 11D and 11E), and in the caudal portion of the dentate nucleus (Fig. 11E and 11F). The latter were located in the wing of the dentate that is adjacent to the PIN. Premotor neurons labeled at shorter survival times have been observed at just three sites following rabies virus injections of the ciliary muscle: the SOA, the cMRF and in the tectal longitudinal column, which lies along the midline between the superior colliculi (May et al., 2018a; 2018b; 2019). At all three sites, the labeling was bilateral, with no clear preference for side; so, it is not surprising that the distribution of labeled neurons that provide these premotor cells with input, is also bilateral. In this case, labeled cells formed clusters of multipolar neurons within the FN (Fig. 12A) and PIN (Fig. 12B) whose somatic long axes were generally around 20 μm

across. Particularly within the PIN, it appeared that nearly all the cells within the cluster were labeled. The second case (not illustrated) displayed fewer labeled cells, but they were located in the same nuclei.

cMRF injection experiments

It was possible that the labeling of cerebellar cells by the rabies injections was entirely due to the known projection by the deep cerebellar nuclei to the SOA (May et al., 1992), and not due to projections to the cMRF. To test this, we injected the cMRF with WGA-HRP. The illustrated injection site was located in the caudal cMRF (Fig. 13A–13C), and tracer diffused along the needle tract to include portions of the pulvinar and pretectum. Lighter spread from this region slightly involved the rostral pole of the superior colliculus. The retrogradely labeled neurons formed a small bilateral cluster in the FN (Fig. 13E–13H). There was also a cluster of neurons located in the ventrolateral portion of the PIN (Fig. 13D–13H). This population was almost entirely contralateral. Finally, retrogradely labeled cells were observed in the wing of the contralateral dentate nucleus that is adjacent to the PIN (Fig. 13F–13H). Thus, the patterns of trans-synaptic label (Fig. 11) and retrograde labeling (Fig. 13) were quite similar.

Discussion

The results we observed indicate that the FN projects bilaterally to both the SOA and cMRF, while the projection of the PIN to the cMRF is primarily contralateral. The specific targets of the fastigial projection to the SOA are likely to include the dendrites of medial rectus MIF motoneurons in the C-group and levator motoneurons, as these connections were seen in all three animals we tested. However, this direct projection is relatively modest, and does not include all the motoneurons in either population, suggesting it has just a modulatory role on the activity of these muscles. There is no projection to superior rectus motoneurons. However, there is a subpopulation of cells in the SOA and the cMRF which receive extensive inputs from the FN indicating their activity is significantly influenced by the cerebellum. The very similar pattern of trans-synaptic labeling of lens accommodation-related neurons in the deep cerebellar nuclei (Fig. 11) and patterns of retrograde labeling following injections of the SOA (May et al., 1992) or the cMRF (Fig. 13) suggest that the labeled regions of these nuclei modulate the near triad. It is thus likely that the cells receiving intensive fastigial terminal input are near response premotor neurons that in turn supply EWpg and medial rectus motoneurons. Therefore, it appears likely that cell populations in the FN and PIN are connected to and modulate the activity of premotor populations controlling lens accommodation and vergence, allowing the eyes to compensate for target distance.

Technical considerations

It needs to be remembered that many exiting fastigial axons cross through the opposite FN. Thus, it is possible that a portion of the ipsilateral labeling observed after fastigial BDA injections may have actually been due to uptake by crossing fibers of passage. Nevertheless, injections of the SOA (May et al., 1992) and the cMRF (Fig. 13) produce bilateral labeling of the FN. As we have noted in Results, there was tracer spread to other extraocular muscles in some cases. This means that the MIF motoneurons in C-group that received

close associations from cerebellar boutons may supply either the medial rectus or inferior rectus muscles (Wasicky et al., 2004). Based on the distribution of their dendrites, it appears that most were medial rectus MIF motoneurons, as relatively few dendrites were observed crossing the midline, as has been described for inferior rectus MIF motoneurons (Tang et al., 2015). With respect to the rabies experiments, the specificity of the uptake by ciliary muscle afferents was insured by finding no labeled cells in cranial ganglia other than the ciliary, and no labeled cells in the olivary pretectal nucleus. (See May et al., 2018b for details.) In the case of the cMRF injections, light tracer spread into the rostral superior colliculus could cloud the issue, as the FN projects bilaterally to this region (May et al., 1990). However, the presence of terminals in the cMRF following cerebellar nuclei injections indicates that at least a portion of the retrogradely labeled neurons observed in the cerebellum project to the cMRF.

In this study, we have demonstrated that fastigial axons display boutons that are in close association with some medial rectus MIF motoneurons and some levator motoneurons. While close associations are suggestive of synaptic contacts, it is also possible that these boutons just lie adjacent to the cell, and no synaptic contact is present. Indeed, a recent trans-synaptic transport study of cerebellar pathways to the lateral rectus muscle indicates that there is no direct synaptic contact with lateral rectus motoneurons (Prevosto et al., 2017). Similarly, we saw no evidence from our rabies cases that cerebellar neurons project directly to EWpg motoneurons, as they were not labeled at the shorter survival times when premotor cells were labeled (May et al., 2018b, 2019), even though numerous terminals are present within EWpg following cerebellar injections (May et al., 1992). On the other hand, it is possible that primate lateral and medial rectus MIF motoneurons are different enough in their functions that they differ in their cerebellar inputs.

C-group

The C-group contains motoneurons supplying medial and inferior rectus MIFs. MIFs not only differ in their innervation pattern, they also display a cellular organization and molecular characteristics that support slower, more sustained action (Spencer & Porter, 2006). For instance, they do not display all or none activation, like SIFs, but are instead capable of graded responses to activity in the axons that make multiple boutonal contacts along their length (Chiarandini & Stefani, 1979; Jacoby et al., 1989). The MIF motoneurons that supply these fibers have different characteristics than the SIF motoneurons. MIF motoneurons are generally smaller (Büttner-Ennever et al., 2001; Erichsen et al., 2014; Bohlen et al., 2017b), display far fewer axosomatic contacts (Erichsen et al., 2014) and show distinctive histochemical profile in that they lack perineuronal nets (Eberhorn et al., 2005, 2006). In view of these differences, it has been suggested that MIF and SIF motoneurons play different functional roles and receive different inputs. In support of this, the dendrites of the C-group motoneurons are largely confined to the SOA, while those of medial rectus SIF motoneurons generally avoid this area (Erichsen et al., 2014; Tang et al., 2015). They also appear to differ in their inputs, as there is evidence that C-group motoneurons are particularly targeted by the pretectum and cMRF (Wasicky et al., 2004; Bohlen et al., 2017a). The present data suggest that they, and not the SIF motoneurons in III, may also receive direct input from the FN. Perhaps the divergence observed following FN inactivation

(Joshi & Das, 2013) is due to loss of FN convergence input (Zhang & Gamlin, 1996) to these medial rectus MIF motoneurons. It should be noted that the functional division between the SIF and MIF motoneuron types is not sharp. Investigation of the activity of MIF motoneurons in the cat indicates that they take part in all types of eye movement (Hernández et al., 2019). They do differ in that the MIF motoneurons have lower firing rates, recruitment thresholds and velocity and position sensitivities. This pattern of partial differences is supported by the fact that both medial rectus MIF and SIF motoneurons receive some input from the vestibular nuclei and from abducens internuclear neurons (Büttner-Ennever & Akert, 1981; Wasicky et al., 2004, although see McCrea et al., 1986). The present data suggest a modest FN input as well.

Cerebellar control of eyelids

Closure of the eyelid in a blink is produced by activation of the orbicularis oculi muscle, whose motoneurons are located in the facial nucleus (Porter et al., 1989; Evinger et al., 1991; Bour et al., 2000). During this action, the levator muscle, which normally holds the eye open for unimpeded vision, must be inhibited (May et al., 2012; Becker & Fuchs, 1988). At the end of the blink, the reactivated levator produces the up-phase. In addition, the levator moves the eyelid in parallel with vertical eye movements (Becker & Fuchs, 1988). We observed close associations between labeled fastigial boutons and levator motoneuron dendrites suggestive of synaptic contact. The cerebellum is known to modulate the blink reflex, as part of conditioned learning (Delgado-García & Gruart, 2002; Chen & Evinger, 2006). There is evidence that the PIN projects directly to some facial motoneurons (Fanardjian & Manvelyan, 1984), but the connections between the cerebellum and orbicularis oculi muscles appear to be indirect (N.B.: direct projections were not seen here), passing by way of interposed nuclei projections to the red nucleus (Sun, 2012; Gonzalez-Joekes & Schreurs, 2012). The up-phase of the blink is regulated by the dorsal portion of the PIN (Sánchez-Campusano et al., 2012), possibly via projections to levator motoneurons, and we saw somewhat denser projections to levator motoneurons when the PIN was involved in the BDA injection (Figs. 1, 4, and 5). The input observed here following FN injections is more likely related to regulating the vertical gaze actions of levator motoneurons than those related to blink, since this region of the deep cerebellar nuclei contains eye movement-related neurons, although mostly horizontal gaze activity has been recorded (Fuchs et al., 1993,1994; Quinet & Goffart, 2007; Quinet & Goffart, 2009). So, the terminals observed here may modulate the vertical gaze activity conferred on levator motoneurons by inputs from the M group of the rostral interstitial nucleus of the medial longitudinal fasciculus and the interstitial nucleus of Cajal (cat: Chen & May, 2002; May et al., 2002; Chen & May, 2007; monkey: Horn & Büttner-Ennever, 2008). Perhaps the cerebellar input helps adjust the vertical movements of the eyelid so that it sits precisely at the pupillary margin during these movements. It is interesting that cerebellar control over vertical eye movements is exercised through input to the vertical gaze centers (Gonzalo-Ruiz et al., 1990; Noda et al., 1990), not the motoneurons for vertical eye movements (present data). Perhaps this is because the vertical eye muscles have secondary actions, but levator does not, making direct input to levator motoneurons possible. Other upgaze inputs to levator motoneurons have been characterized by the presence of calretinin (Zeeh et al., 2013;

Adamczyk et al., 2015). It would be interesting to see if such a population is present in the cerebellar nuclei.

Cerebellar control over the near response

It is clear that most of the cerebellar terminals labeled in the SOA were not directed at the motoneuron populations tested here or at EWpg motoneurons. There are only two other known occupants of the SOA, midbrain near response neurons, and peptidergic cells belonging to the EWcp population. The latter have diffuse projections throughout the brain (Horn et al., 2008; May et al., 2008; Kozicz et al., 2011), and appear to be involved in eating and drinking behavior, and perhaps stress responses (Ryabinin & Weitemier, 2006; Weitemier & Ryabinin, 2006; Kozicz et al., 2011). As the regions of the deep cerebellar nuclei that provide input to the SOA are known to be largely involved in eye movement control (Gardner & Fuchs, 1975; Hepp et al., 1982; May et al., 1990), it seems unlikely that they provide a major input to peptidergic EWcp cells. So, we would conclude that the target of the FN terminals we observed in the SOA is probably the near response population.

The cerebellar projections to the SOA observed in the present study are similar to those observed previously with other tracers (rat: Gonzalo-Ruiz et al., 1990; monkey: Gonzalo-Ruiz et al., 1988; Gonzalo-Ruiz & Leichnetz, 1990; May et al., 1992). However, this is the first study to provide a detailed view of the fastigial axon terminal arbors, and the fact they sometimes terminate extremely densely on a subpopulation of cells. It seems most likely that these SOA cells are near response neurons. The vergence-related activity of near response neurons in SOA has been characterized in a number of studies (Mays, 1984; Judge & Cumming, 1986; Zhang et al., 1992; Das, 2011, 2012; Pallus et al., 2018a, 2018b), and it appears that they produce dynamic and tonic signals used to change and maintain the vergence angle, respectively. They were originally named near response neurons as most appeared to be tuned for near targets, and relatively few were tuned for far viewing. With respect to the present results, it should be noted that unilateral injections of muscimol into the near-response region of the posterior FN localized with single-unit recording and microstimulation results in consistent deficits in the ability of the animal to generate and maintain convergence and accommodation. These animals displayed significant vergence insufficiency and accommodative responses were almost eliminated (Gamlin & Zhang, 1996). If the FN projection normally provides an excitatory drive to convergence neurons, which represent the majority of near response cells in the SOA, this would explain why FN inactivation leads to divergence (Joshi & Das, 2013). A significant number of near response cells also fire in relation to lens accommodation (Judge & Cumming, 1986; Zhang et al., 1992; Gamlin et al., 1994). We have anatomically defined the lens-related SOA population using trans-synaptic transport of rabies virus (May et al., 2018b) and their location corresponds to the fastigial terminal field seen here. More specifically, the cells that were heavily encrusted with terminals in the present study lie within the area of the SOA where we demonstrated premotor neurons supporting lens accommodation, and their size and primary dendritic organization also appear similar (May et al., 2018b). So, these neurons are likely to be interneurons for cerebellar control over the near response. The idea that the activity of these cells is modulated by cerebellar inputs makes sense, in that vergence-related activity has been recorded in essentially the same regions of the caudal FN and PIN (Zhang

& Gamlin, 1996; Zhang & Gamlin, 1998) where we found trans-synaptically labeled lens accommodation-related cells in the present study. Furthermore, the same areas contain SOA input cells (May et al., 1992). In the future, it will be interesting to test how adaptation of the vergence and accommodation responses might change the activity of these cerebellar neurons and their SOA targets.

We also have evidence from the present study that these regions of the cerebellar nuclei also supply input to the cMRF. By use of other methods, previous studies have noted the presence of terminal fields in the reticular formation lateral to III that originate from the FN (cat: Angaut & Bowsher, 1970; dog: Person et al., 1986; monkey: Batton et al., 1977) and PIN (cat: Kawamura et al., 1982; monkey: Stanton, 1980). However, this is the first study to demonstrate the morphology of the cMRF axonal arbors from the FN and the special relationship they have with a subpopulation of target neurons. We have previously demonstrated that premotor neurons controlling lens accommodation are widely, and bilaterally, distributed in the cMRF (May et al., 2019; May & Gamlin, 2020). Based on the similarities between the morphology of these cMRF premotor neurons and the cells heavily encrusted with terminals, it is likely that they represent interneurons whose near response activity is modulated by cerebellar input. Lens accommodation has not been specifically addressed in physiological studies of the cMRF. However, burst-tonic neurons coding for symmetric vergence eye movements have been recorded in the medial cMRF, adjacent to the medial longitudinal fasciculus (Mays et al., 1986). In addition, neurons whose firing is primarily tied to movements of one eye have been described in the cMRF (Waitzman et al., 2008). The activity of these long lead burst neurons appears to be modulated for disjunctive saccades, in which a saccade is made between targets lying at different distances from the viewer. We recently discovered a third population in the cMRF termed saccade vergence burst neurons (Quinet et al., 2020). These cells only fire during disjunctive saccades, and do not fire for conjugate saccades or symmetric vergence movements. All of these physiological cell types represent potential targets of the projections from the FN and PIN. The fact that FN inactivation particularly affects vergence velocity (Gamlin & Zhang, 1996), and the cells with dense synaptic input were found within the part of the cMRF where vergence velocity burst neurons are located (Mays et al., 1986) may be telling in this regard. In summary, the targets of the cerebellar nuclear projection likely include neurons that transmit vergence signals, lens accommodation signals and signals related to saccades onto the cMRF. Future studies may determine which cells are targeted and how they are influenced.

Acknowledgments.

We would like to express our appreciation to Dr. Isabelle Billig, and the staff of the Systems Neuroscience Institute and the Center for Neuroanatomy with Neurotropic Viruses at the University of Pittsburgh Medical Center, and to their director, Dr. Peter Strick, for their critical support in the rabies experiments. We are also indebted to Dr. Matthias Schnell of Thomas Jefferson University for the antibodies to the rabies virus. Jinrong Wei provided her usual excellent technical support at the University of Mississippi Medical Center. The initial analysis of the rabies data was undertaken by two undergraduate summer students: Hannah Tran and K. Ford Gordon.

Funding Statement.

This research was made possible by NIH grant EY014263 to P.J.M., P.D.G., and S.W.

Abbreviations:

AIN	anterior interposed nucleus
BDA	biotinylated dextran amine
CC	caudal central subdivision of III
CG	central gray
cMRF	central mesencephalic reticular formation
DN	dentate nucleus
EWpg	preganglionic Edinger–Westphal nucleus
FN	fastigial nucleus
III	oculomotor nucleus
InC	interstitial nucleus of Cajal
LGN	lateral geniculate nucleus
MD	medial dorsal nucleus
MLF	medial longitudinal fasciculus
nPC	nucleus of the posterior commissure
PC	posterior commissure
piMRF	peri-interstial nucleus of Cajal portion of the mesencephalic reticular formation
PIN	posterior interposed nucleus
PRF	pontine reticular formation
Pt	pretectum
SOA	supraoculomotor area
WGA-HRP	wheat germ agglutinin conjugated horseradish peroxidase

References

Adamczyk C, Strupp M, Jahn K & Horn AK (2015). Calretinin as a marker for premotor neurons involved in upgaze in human brainstem. Frontiers in Neuroanatomy 9, 153. doi:10.3389/fnana.2015.00153. [PubMed: 26696837]

Angaut P & Bowsher D (1970). Ascending projections of the medial cerebellar (fastigial) nucleus: An experimental study in the cat. Brain Research 24,49–68. [PubMed: 5503234]

Bando T, Ishihara A & Tsukahara N (1979). Interpositus neurons controlling lens accommodation. Proceedings of the Japanese Academy 55, 153–156.

Bando T, Tsukuda K, Yamamoto N, Maeda J & Tsukahara N (1984). Physiological identification of midbrain neurons related to lens accommodation in cats. Journal of Neurophysiology 52, 870–878. [PubMed: 6512591]

Barash S, Melikyan A, Sivakov A, Zhang M, Glickstein M & Thier P (1999). Saccadic dysmetria and adaptation after lesions of the cerebellar cortex. Journal of Neuroscience 19, 10931–10939. [PubMed: 10594074]

Batton RR III, Jayaraman A, Ruggiero D & Carpenter MB (1977). Fastigial efferent projections in the monkey: An autoradiographic study. Journal of Comparative Neurology 174, 281–305.

Becker W & Fuchs AF (1988). Lid-eye coordination during vertical gaze changes in man and monkey. Journal of Neurophysiology 60, 1227–1252. [PubMed: 3193155]

Bohlen MO, Warren S & May PJ (2017a). A central mesencephalic reticular formation projection to medial rectus motoneurons supplying singly and multiply innervated extraocular muscle fibers. Journal of Comparative Neurology 525, 2000–2018.

Bohlen MO, Warren S, Mustari MJ & May PJ (2017b). Examination of feline extraocular motoneuron pools as a function of muscle fiber innervation type and muscle layer. Journal of Comparative Neurology 525, 919–935.

Bour LJ, Aramideh M & de Visser BW (2000). Neurophysiological aspects of eye and eyelid movements during blinking in humans. Journal of Neurophysiology 83, 166–176. [PubMed: 10634863]

Bourrelly C, Quinet J & Goffart L (2018). Pursuit disorder and saccade dysmetria after caudal fastigial inactivation in the monkey. Journal of Neurophysiology 120, 1640–1654. doi:10.1152/jn.00278.2018. [PubMed: 29995606]

Büttner-Ennever JA & Akert K (1981). Medial rectus subgroups of the oculomotor nucleus and their abducens internuclear input in the monkey. Journal of Comparative Neurology 197, 17–27.

Büttner-Ennever JA, Horn AK, Scherberger H & D'Ascanio P (2001). Motoneurons of twitch and nontwitch extraocular muscle fibers in the abducens, trochlear, and oculomotor nuclei of monkeys. Journal of Comparative Neurology 438, 318–335.

Chaturvedi V & van Gisbergen JA (1997). Specificity of saccadic adaptation in three-dimensional space. Vision Research 37, 1367–1382. [PubMed: 9205728]

Chen B & May PJ (2002). Premotor circuits controlling eyelid movements in conjunction with vertical saccades in the cat: I. The rostral interstitial nucleus of the medial longitudinal fasciculus. Journal of Comparative Neurology 450, 183–202.

Chen B & May PJ (2007). Premotor circuits controlling eyelid movements in conjunction with vertical saccades in the cat: II. Interstitial nucleus of Cajal. Journal of Comparative Neurology 500, 676–692.

Chen FP & Evinger C (2006). Cerebellar modulation of trigeminal reflex blinks: Interpositus neurons. Journal of Neuroscience 26, 10569–10576. [PubMed: 17035543]

Chiarandini DJ & Stefani E (1979). Electrophysiological identification of two types of fibres in rat extraocular muscles. Journal of Physiology 290, 453–465.

Das VE (2011). Cells in the supraoculomotor area in monkeys with strabismus show activity related to the strabismus angle. Annals of the New York Academy of Science 1233, 85–90.

Das VE (2012). Responses of cells in the midbrain near-response area in monkeys with strabismus. Investigative Ophthalmology and Visual Science 53, 3858–3864. [PubMed: 22562519]

Dash S & Thier P (2014). Cerebellum-dependent motor learning: Lessons from adaptation of eye movements in primates. Progress in Brain Research 210, 121–155. [PubMed: 24916292]

Delgado-García JM & Gruart A (2002). The role of interpositus nucleus in eyelid conditioned responses. Cerebellum 1, 289–308. [PubMed: 12879967]

Eberhorn AC, Ardeleanu P, Büttner-Ennever JA & Horn AK (2005). Histochemical differences between motoneurons supplying multiply and singly innervated extraocular muscle fibers. Journal of Comparative Neurology 491, 352–366.

Eberhorn AC, Büttner-Ennever JA & Horn AK (2006). Identification of motoneurons supplying multiply- or singly-innervated extraocular muscle fibers in the rat. Neuroscience 137, 891–903. [PubMed: 16330150]

Edwards SB & Henkel CK (1978). Superior colliculus connections with the extraocular motor nuclei in the cat. Journal of Comparative Neurology 179, 451–467.

Erichsen JT, Wright NF & May PJ (2014). Morphology and ultrastructure of medial rectus subgroup motoneurons in the macaque monkey. Journal of Comparative Neurology 522, 626–641.

Erkelens IM, Bobier WR, Macmillan AC, Maione NL, Martin Calderon C, Patterson H & Thompson B (2020). A differential role for the posterior cerebellum in the adaptive control of convergence eye movements. Brain Stimulation 13, 215–228. [PubMed: 31427273]

Evinger C, Manning KA & Sibony PA (1991). Eyelid movements. Mechanisms and normal data. Investigative Ophthalmology and Visual Science 32, 387–400. [PubMed: 1993591]

Fanardjian VV &Manvelyan LR (1984). Peculiarities of cerebellar excitation of facial nucleus motoneurons. Neuroscience Letters 49, 265–270. [PubMed: 6493608]

Fuchs AF, Robinson FR & Straube A (1993). Role of the caudal fastigial in saccade generation. I. Neuronal discharge pattern. Journal of Neurophysiology 70, 1723–1740, 1993. [PubMed: 8294949]

Fuchs AF, Robinson FR & Straube A (1994). Participation of the caudal fastigial nucleus in smooth-pursuit eye movements. I. Neuronal activity. Journal of Neurophysiology 72, 2714–2728. [PubMed: 7897484]

Gamlin PD, Zhang Y, Clendaniel RA & Mays LE (1994). Behavior of identified Edinger-Westphal neurons during ocular accommodation. Journal of Neurophysiology 72, 2368–2382. [PubMed: 7884465]

Gamlin PDR & Zhang HY (1996). Effects of muscimol blockade of the posterior fastigial nucleus on vergence and ocular accommodation in the primate. Society for Neuroscience Abstracts 22, 2034.

Gardner EP & Fuchs AF (1975). Single-unit responses to natural vestibular stimuli and eye movements in deep cerebellar nuclei of the alert rhesus monkey. Journal of Neurophysiology 38, 627–649. [PubMed: 1079240]

Gonzalez-Joekes J & Schreurs BG (2012). Anatomical characterization of a rabbit cerebellar eyeblink premotor pathway using pseudorabies and identification of a local modulatory network in anterior interpositus. Journal of Neuroscience 32, 12472–12487. [PubMed: 22956838]

Gonzalo-Ruiz A & Leichnetz GR (1990). Connections of the caudal cerebellar interpositus complex in a New World monkey (Cebus apella). Brain Research Bulletin 25, 919–927. [PubMed: 2289174]

Gonzalo-Ruiz A, Leichnetz GR & Hardy SG (1990). Projections of the medial cerebellar nucleus to oculomotor-related midbrain areas in the rat: An anterograde and retrograde HRP study. Journal of Comparative Neurology 296, 427–436.

Gonzalo-Ruiz A, Leichnetz GR & Smith DJ (1988). Origin of cerebellar projections to the region of the oculomotor complex, medial pontine reticular formation, and superior colliculus in New World monkeys: A retrograde horseradish peroxidase study. Journal of Comparative Neurology 268, 508–526.

Hepp K, Henn V & Jaeger J (1982). Eye movement related neurons in the cerebellar nuclei of the alert monkey. Experimental Brain Research 45, 253–264. [PubMed: 7056331]

Hernández RG, Calvo PM, Blumer R, de la Cruz RR & Pastor AM (2019). Functional diversity of motoneurons in the oculomotor system. Proceedings of the National Academy of Science USA 116, 3837–3846.

Hopp JJ & Fuchs AF (2004). The characteristics and neuronal substrate of saccadic eye movement plasticity. Progress in Neurobiology 72, 27–53. [PubMed: 15019175]

Horn AK, Eberhorn A, Härtig W, Ardeleanu P, Messoudi A & Büttner-Ennever JA (2008). Perioculomotor cell groups in monkey and man defined by their histochemical and functional properties: Reappraisal of the Edinger-Westphal nucleus. Journal of Comparative Neurology 507, 1317–1335.

Horn AKE & Büttner-Ennever JA (2008). Brainstem circuits controlling lid-eye coordination in monkey. Progress in Brain Research 171, 87–95. doi: 10.1016/S0079-123(08)00612-2. [PubMed: 18718286]

Hosoba M, Bando T & Tsukahara N (1978). The cerebellar control of accommodation of the eye in the cat. Brain Research 153, 495–505. [PubMed: 698790]

Iwamoto Y & Kaku Y (2010). Saccade adaptation as a model of learning in voluntary movements. Experimental Brain Research 204, 145–162. doi:10.1007/s00221-010-2314-3. [PubMed: 20544185]

Jacoby J, Chiarandini DJ & Stefani E (1989). Electrical properties and innervation of fibers in the orbital layer of rat extraocular muscles. Journal of Neurophysiology 61, 116–125. [PubMed: 2783961]

Joshi AC & Das VE (2013). Muscimol inactivation of caudal fastigial nucleus. Journal of Neurophysiology 110, 1882–1891. [PubMed: 23883862]

Judge SJ & Cumming BG (1986). Neurons in the monkey midbrain with activity related to vergence eye movement and accommodation. Journal of Neurophysiology 55, 915–930. [PubMed: 3711972]

Kawamura S, Hattori S, Higo S & Matsuyama T (1982). The cerebellar projections to the superior colliculus and pretectum in the cat: An autoradiographic and horseradish peroxidase study. Neuroscience 7, 1673–1689. [PubMed: 7121831]

Kim G, Laurens J, Yakusheva TA & Blazquez PM (2019). The macaque cerebellar flocculus outputs a forward model of eye movement. Frontiers in Integrative Neuroscience 13, 12. [PubMed: 31024268]

Kojima Y, Soetedjo R & Fuchs AF (2011). Effect of inactivation and disinhibition of the oculomotor vermis on saccade adaptation. Brain Research 1401, 30–39. [PubMed: 21679930]

Kozicz T, Bittencourt JC, May PJ, Reiner A, Gamlin PD, Palkovits M, Horn AK, Toledo CA & Ryabinin AE (2011). The Edinger-Westphal nucleus: A historical, structural, and functional perspective on a dichotomous terminology. Journal of Comparative Neurology 519, 1413–1434.

Leigh RJ & Zee DS (2015). The Neurology of Eye Movements (5th ed.). Oxford, UK: Oxford University Press, pp. 520–568.

Lisberger SG (2010). Visual guidance of smooth-pursuit eye movements: Sensation, action, and what happens in between. Neuron 66, 477–491. doi: 10.1016/j.neuron.2010.03.027. [PubMed: 20510853]

Lv X, Chen Y, Tan W, Yu Y, Zou H, Shao Y, Zan S, Tao J & Miao W (2020). Functional neuroanatomy of the human accommodation response to an “E” target varying from −3 to −6 diopters. Frontiers in Integrative Neuroscience 14, 29. [PubMed: 32508603]

Maxwell JS & Schor CM (1994). Mechanisms of vertical phoria adaptation revealed by time-course and two-dimensional spatiotopic maps. Vision Research 34, 241–251. [PubMed: 8116283]

May PJ, Baker RG & Chen B (2002). The eyelid levator muscle: Servant of two masters. Movement Disorders 17(Suppl 2), S4–S7. [PubMed: 11836743]

May PJ, Billig I, Gamlin PD & Quinet J (2019). Central mesencephalic reticular formation control of the near response: Lens accommodation circuits. Journal of Neurophysiology 21, 1692–1703.

May PJ & Gamlin PD (2020). Is primate lens accommodation unilaterally or bilaterally controlled? Investigative Ophthalmology and Visual Science 61,5.

May PJ, Hartwich-Young R, Nelson J, Sparks DL & Porter JD (1990). Cerebellotectal pathways in the macaque: Implications for collicular generation of saccades. Neuroscience 36, 305–324. [PubMed: 2215926]

May PJ, Porter JD & Gamlin PD (1992). Interconnections between the primate cerebellum and midbrain near-response regions. Journal of Comparative Neurology 315, 98–116.

May PJ, Reiner AJ & Ryabinin AE (2008). Comparison of the distributions of urocortin-containing and cholinergic neurons in the perioculomotor midbrain of the cat and macaque. Journal of Comparative Neurology 507, 1300–1316.

May PJ, Vidal P-P, Baker H & Baker R (2012). Physiological and anatomical evidence for an inhibitory trigemino-oculomotor pathway in the cat. Journal of Comparative Neurology 520, 2218–2240.

May PJ, Warren S, Billig I, Quinet JJ & Gamlin PD (2018a). A new tectal premotor input for the control of lens accommodation. Society for Neuroscience Abstracts 44, 398.07.

May PJ, Warren S, Gamlin PD & Billig I (2018b). An anatomic characterization of the midbrain near response neurons in the macaque monkey. Investigative Ophthalmology and Visual Science 59, 1486–1502. [PubMed: 29625471]

Mays LE (1984). Neural control of vergence eye movements: Convergence and divergence neurons in midbrain. Journal of Neurophysiology 51, 1091–1108. [PubMed: 6726313]

Mays LE, Porter JD, Gamlin PDR & Tello CA (1986). Neural control of vergence eye movements: Neurons encoding vergence velocity. Journal of Neurophysiology 56, 1007–1021. [PubMed: 3783225]

McCann BC, Hayhoe MM & Geisler WS (2018). Contributions of monocular and binocular cues to distance discrimination in natural scenes. Journal of Vision 18, 1–15.

McCrea RA, Strassman A & Highstein SM (1986). Morphology and physiology of abducens motoneurons and internuclear neurons intracellularly injected with horseradish peroxidase in alert squirrel monkeys. Journal of Comparative Neurology 243, 291–308. doi:10.1002/cne.902430302.

Milder DG & Reinecke RD (1983). Phoria adaptation to prisms. A cerebellar-dependent response. Archives of Neurology 40, 339–342. [PubMed: 6847437]

Nitta T, Akao T, Kurkin S & Fukushima K (2008). Involvement of the cerebellar dorsal vermis in vergence eye movements in monkeys. Cerebral Cortex 18, 1042–1057. doi:10.1093/cercor/bhm143. [PubMed: 17716988]

Noda H, Sugita S & Ikeda Y (1990). Afferent and efferent connections of the oculomotor region of the fastigial nucleus in the macaque monkey. Journal of Comparative Neurology 302, 330–348. doi:10.1002/cne.903020211.

Pallus AC, Walton MMG & Mustari MJ (2018a). Response of supraoculomotor area neurons during combined saccade-vergence movements. Journal of Neurophysiology 119, 585–596. [PubMed: 29142092]

Pallus A, Walton MMG & Mustari M (2018b). Activity of near-response cells during disconjugate saccades in strabismic monkeys. Journal of Neurophysiology 120, 2282–2295. [PubMed: 30110234]

Paxinos G, Huang X-F & Toga AW (2000). The Rhesus Monkey Brain in Stereotaxic Coordinates. San Diego: Academic Press.

Person RJ, Andrezik JA, Dormer KJ & Foreman RD (1986). Fastigial nucleus projections in the midbrain and thalamus in dogs. Neuroscience 18, 105–120. [PubMed: 2426627]

Porter JD, Burns LA & May PJ (1989). Morphological substrate for eyelid movements: Innervation and structure of primate levator palpebrae superioris and orbicularis oculi muscles. Journal of Comparative Neurology 287, 64–81.

Prevosto V, Graf W & Ugolini G (2017). The control of eye movements by the cerebellar nuclei: Polysynaptic projections from the fastigial, interpositus posterior and dentate nuclei to lateral rectus motoneurons in primates. European Journal of Neuroscience 45, 1538–1552.

Quinet J & Goffart L (2007). Head-unrestrained gaze shifts after muscimol injection in the caudal fastigial nucleus of the monkey. Journal of Neurophysiology 98, 3269–3283. doi:10.1152/jn.00741.2007. [PubMed: 17928556]

Quinet J & Goffart L (2009). Electrical microstimulation of the fastigial oculomotor region in the head-unrestrained monkey. Journal of Neurophysiology 102, 320–336. doi: 10.1152/jn.90716.2008. [PubMed: 19439677]

Quinet J, Schultz K, May PJ & Gamlin PD (2020). Neural control of rapid binocular eye movements: Saccade-vergence burst neurons. Proceedings of the National Academy of Science U S A 117, 29123–29132. doi:10.1073/pnas.2015318117.

Raghavan RT & Lisberger SG (2017). Responses of Purkinje cells in the oculomotor vermis of monkeys during smooth pursuit eye movements and saccades: Comparison with floccular complex. Journal of Neurophysiology 118, 986–1001. doi:10.1152/jn.00209.2017. [PubMed: 28515286]

Raux H, Iseni F, Lafay F & Blondel D (1997). Mapping of monoclonal antibody epitopes of the rabies virus P protein. Journal of General Virology 78, 119–124.

Richter HO, Costello P, Sponheim SR, Lee JT & Pardo JV (2004). Functional neuroanatomy of the human near/far response to blur cues: Eye-lens accommodation/vergence to point targets varying in depth. European Journal of Neuroscience 20, 2722–2732.

Richter HO, Lee JT & Pardo JV (2000). Neuroanatomical correlates of the near response: Voluntary modulation of accommodation/vergence in the human visual system. European Journal of Neuroscience 12, 311–321.

Ruigrok TJ, van Touw S & Coulon P (2016). Caveats in transneuronal tracing with unmodified rabies virus: An evaluation of aberrant results using a nearly perfect tracing technique. Frontiers in Neural Circuits 10, 46. [PubMed: 27462206]

Ryabinin AE & Weitemier AZ (2006). The Urocortin 1 neurocircuit: Ethanol-sensitivity and potential involvement in alcohol consumption. Brain Research Reviews 52, 368–380. [PubMed: 16766036]

Sánchez-Campusano R, Gruart A, Fernández-Mas R & Delgado-Garcia JM (2012). An agonist-antagonist cerebellar nuclear system controlling eyelid kinematics during motor learning. Frontiers in Neuroanatomy 6, 8. [PubMed: 22435053]

Sander T, Sprenger A, Neumann G, Machner B, Gottschalk S, Rambold H & Helmchen C (2009). Vergence deficits in patients with cerebellar lesions. Brain 132, 103–115. [PubMed: 19036765]

Schor CM, Maxwell JS, McCandless J & Graf E (2002). Adaptive control of vergence in humans. Annals of the New York Academy of Science 956,297–305.

Schor CM & McCandless JW (1995). An adaptable association between vertical and horizontal vergence. Vision Research 35, 3519–3527. [PubMed: 8560816]

Soetedjo R, Kojima Y & Fuchs AF (2008). Complex spike activity in the oculomotor vermis of the cerebellum: A vectorial error signal for saccade motor learning? Journal of Neurophysiology 100, 1949–1966. [PubMed: 18650308]

Soetedjo R, Kojima Y & Fuchs AF (2019). How cerebellar motor learning keeps saccades accurate. Journal of Neurophysiology 121, 2153–2162. doi: 10.1152/jn.00781.2018. [PubMed: 30995136]

Spencer RF & Porter JD (2006). Biological organization of the extraocular muscles. In Neuroanatomy of the Oculomotor System, Ed. Büttner-Ennever, J.A. Progress in Brain Research 151, 43–80. [PubMed: 16221585]

Stanton GB (1980). Topographical organization of ascending cerebellar projections from the dentate and interposed nuclei in Macaca mulatta: An anterograde degeneration study. Journal of Comparative Neurology 190, 699–731.

Sun LW (2012). Transsynaptic tracing of conditioned eyeblink circuits in the mouse cerebellum. Neuroscience 203, 122–134. [PubMed: 22198021]

Szabo J & Cowan WM (1984). A stereotaxic atlas of the brain of the cynomologous monkey (Macaca fascicularis). Journal of Comparative Neurology 222, 265–300.

Takagi M, Tamargo R & Zee DS (2003). Effects of lesions of the cerebellar oculomotor vermis on eye movements in primate: Binocular control. Progress in Brain Research 142, 19–33. doi: 10.1016/S0079-6123(03)42004-9. [PubMed: 12693252]

Takagi M, Zee DS & Tamargo RJ (2000). Effects of lesions of the oculomotor cerebellar vermis on eye movements in primate: Smooth pursuit. Journal of Neurophysiology 83, 2047–2062. [PubMed: 10758115]

Takeichi N, Kaneko CRS & Fuchs AF (2007). Activity changes in monkey superior colliculus during saccade adaptation. Journal of Neurophysiology 97, 4096–4107. doi: 10.1152/jn.01278.2006. [PubMed: 17442764]

Tang X, Büttner-Ennever JA, Mustari MJ & Horn AKE (2015). Internal organization of medial rectus and inferior rectus muscle neurons in the C group of the oculomotor nucleus in monkey. Journal of Comparative Neurology 523, 1809–1823.

Waitzman DM, Van Horn MR & Cullen KE (2008). Neuronal evidence for individual eye control in the primate cMRF. Progress in Brain Research 171, 143–150. [PubMed: 18718293]

Walton MMG, Pallus A & Mustari M (2019). A rhesus monkey with a naturally occurring impairment of disparity vergence. II. Abnormal near response cell activity in the supraoculomotor area. Investigative Ophthalmology and Visual Science 60, 1670–1676. [PubMed: 30999322]

Wasicky R, Horn AKE & Büttner-Ennever JA (2004). Twitch and nontwitch motoneuron subgroups in the oculomotor nucleus of monkeys receive different afferent projections. Journal of Comparative Neurology 479, 117–129.

Weitemier AZ & Ryabinin AE (2006). Urocortin 1 in the dorsal raphe regulates food and fluid consumption, but not ethanol preference in C57BL/6J mice. Neuroscience 137, 1439–1445. [PubMed: 16338088]

Zeeh C, Hess BJ & Horn AK (2013). Calretinin inputs are confined to motoneurons for upward eye movements in monkey. Journal of Comparative Neurology 521, 3154–3166. doi:10.1002/cne.23337.

Zhang H & Gamlin PD (1996). Single-unit activity within the posterior fastigial nucleus during vergence and accommodation in the alert primate. Society for Neuroscience Abstracts 22, 2034 #801.1.

Zhang H & Gamlin PD (1998). Neurons in the posterior interposed nucleus of the cerebellum related to vergence and accommodation. I. Steady-state characteristics. Journal of Neurophysiology 79, 1255–1269. [PubMed: 9497407]

Zhang Y, Mays LE & Gamlin PD (1992). Characteristics of near response cells projecting to the oculomotor nucleus. Journal of Neurophysiology 67, 944–960. [PubMed: 1588393]

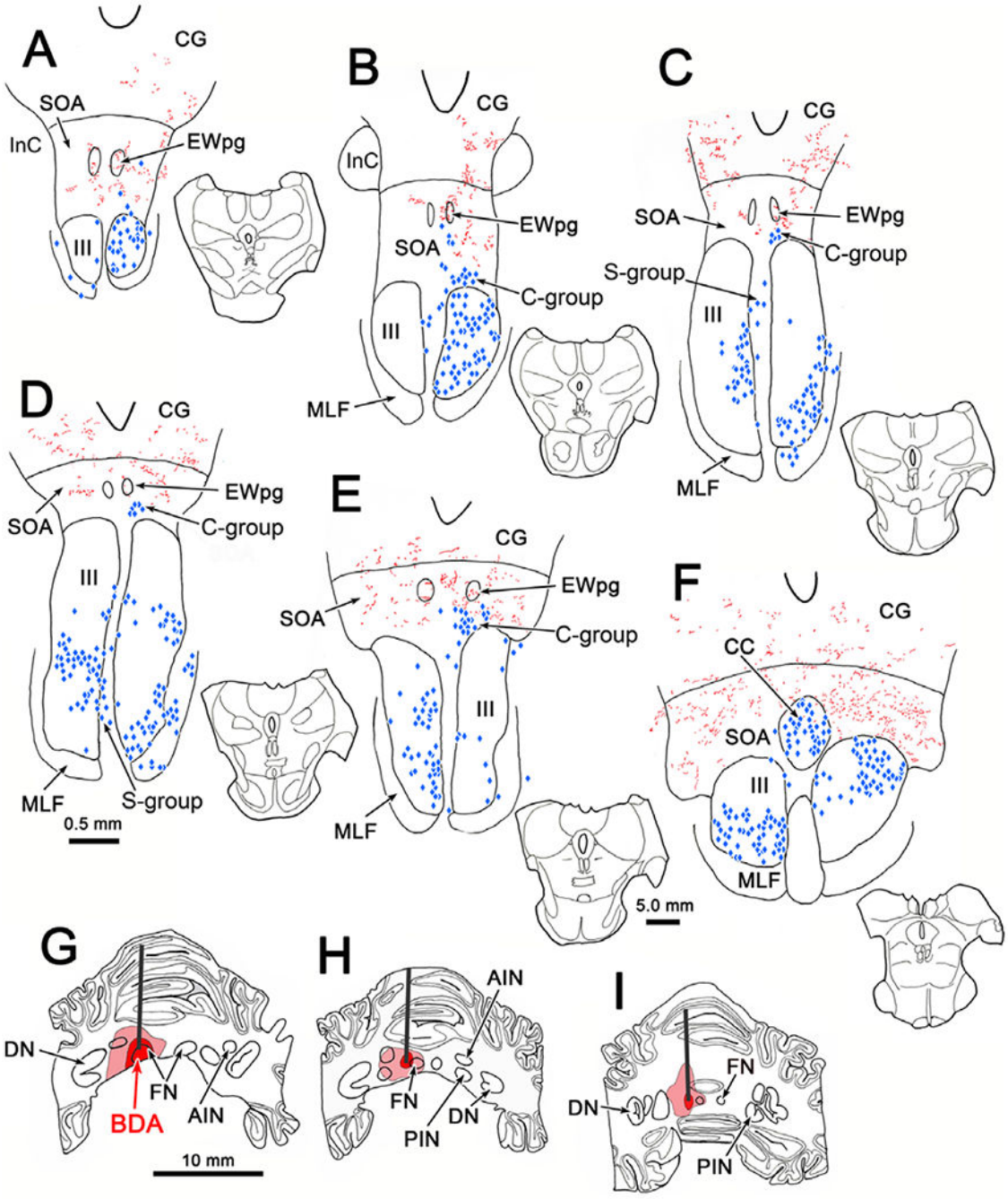

Fig. 1.

Relationship of cerebellar terminals to oculomotor nucleus motoneurons. The BDA injection extended from the left fastigial nucleus (FN) into the left anterior interposed (AIN) and posterior interposed nuclei (PIN) (G–I). (Core of injection site indicated by dark red and spread by lighter red.) BDA labeled axons terminated bilaterally (red), with a contralateral predominance in the supraoculomotor area SOA (A–F). Retrogradely labeled motoneurons (blue diamonds) in the left oculomotor nucleus (III) (C–F) were produced by tracer injections of the right superior rectus muscle. Injections into the right medial rectus muscle

labeled motoneurons in the right III (A–F). Injections into the right levator muscle labeled motoneurons bilaterally in the caudal central subdivision (CC) (F). Overlap between the labeled medial rectus motoneurons and terminals was present in the SOA, where C-group motoneurons are found (B–E), and in the CC (F). Sections are arranged in rostral to caudal order in this and other chartings. Insets indicate section illustrated in this and other chartings.

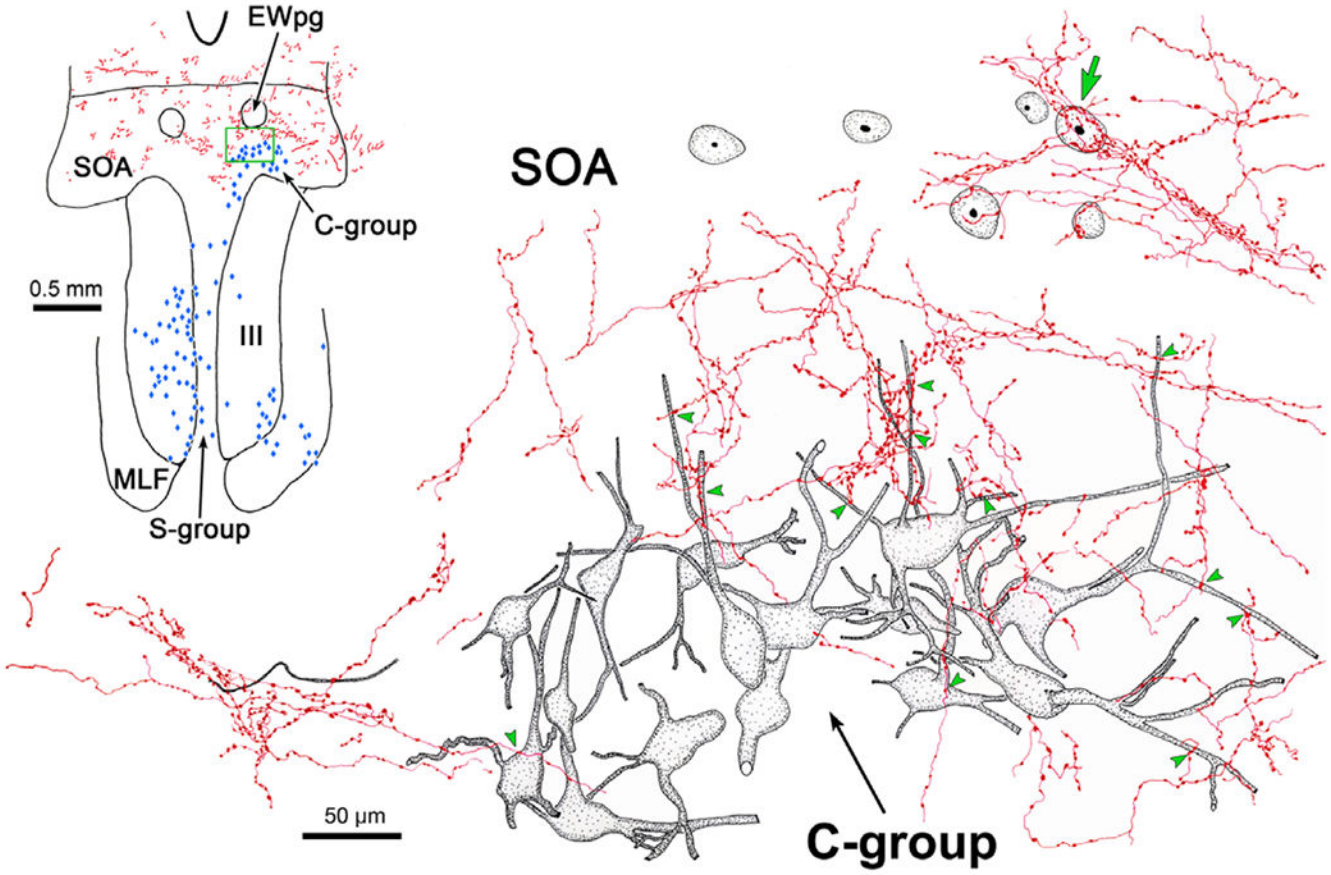

Fig. 2.

Targeting of C-group motoneurons and subpopulation of SOA cells by cerebellar boutons (same case as illustrated in Fig. 1). Anterogradely labeled terminal arbors (red) overlap with the somata and dendrites of some, but not all, of the retrogradely labeled (gray shading) C-group motoneurons. Examples of close associations with boutons indicated by green arrowheads. Within the SOA, a counterstained soma is encrusted with boutons (short arrow) that appear to extend onto the cell's dendrites. Region illustrated at high magnification is indicated by the green box in the inset. Retrogradely labeled neurons are indicated by blue diamonds in inset.

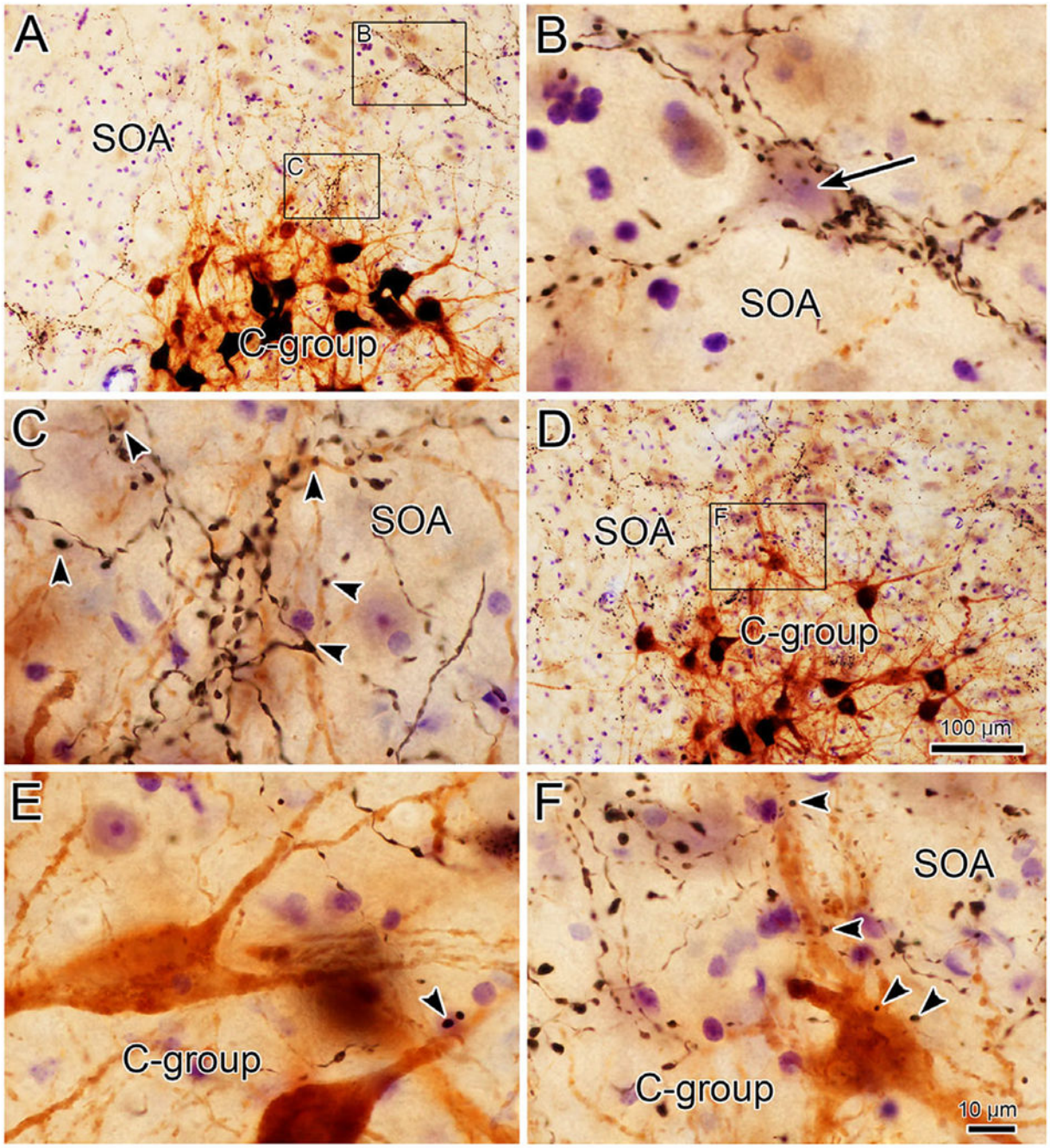

Fig. 3.

Close associations between cerebellar boutons and targets in the SOA. Examples from the case illustrated in Fig. 1. Lower magnification views are shown in A and D where brown MIF motoneurons are visible in the C-group. Boxed areas dorsal to the C-group are shown at higher magnification in C and F. Close associations (arrowheads) are present between BDA labeled boutons and the somata and dendrites of the motoneurons. An additional example is shown in E. Terminal fields in SOA (A), sometimes select a cell (upper boxed region) where

(B) the cell body (short arrow) and dendrites are encrusted with BDA labeled boutons. Scale in D = A; in F = B, C, and E.

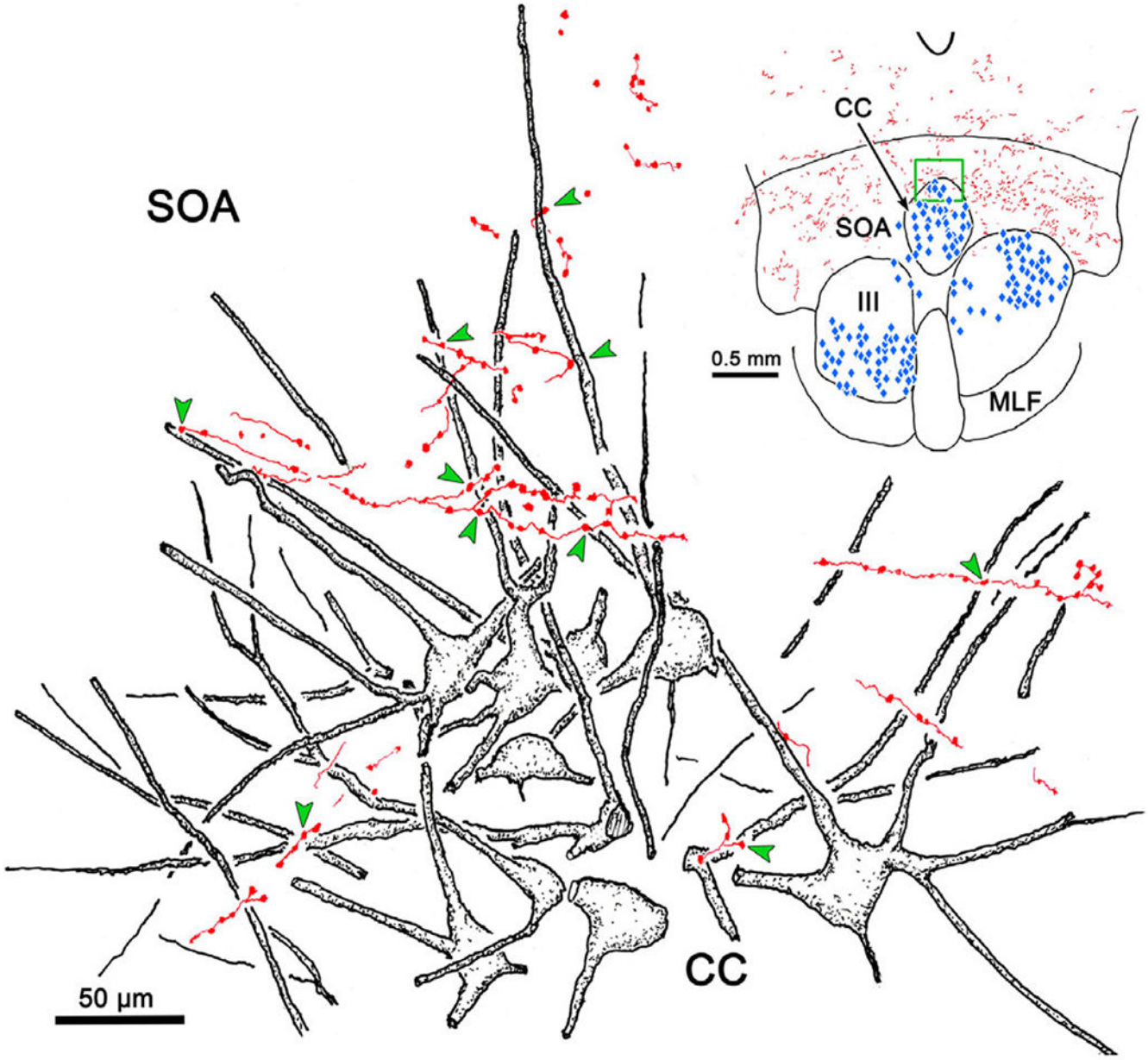

Fig. 4.

Targeting of levator motoneurons by cerebellar boutons (same case as illustrated in Fig. 1). Anterogradely labeled axonal arbors (red) overlap with the dendrites of some, but not all, of the retrogradely labeled levator motoneurons at the dorsal edge of the caudal central subdivision (CC). Examples of close associations with boutons indicated by green arrowheads. The region illustrated at high magnification is indicated by the green box in the inset. Retrogradely labeled neurons are indicated by blue diamonds in inset.

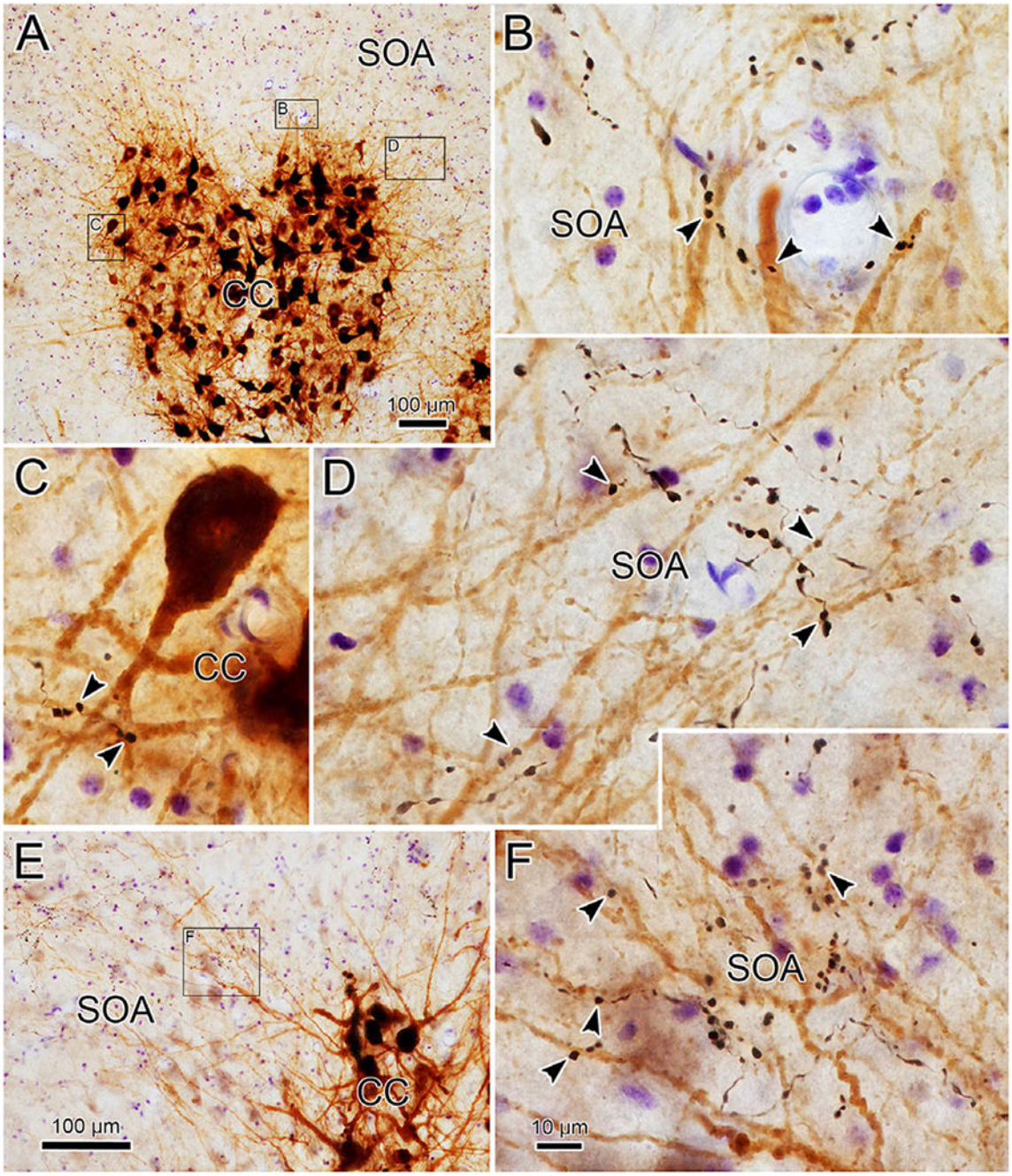

Fig. 5.

Close associations between cerebellar boutons and levator motoneurons (from case illustrated in Fig. 1). Lower magnification view (A) shows labeled motoneurons filling the caudal central subdivision (CC). Boxed areas are shown at higher magnification in B–D (left box—C, middle box—B, right box—D). Close associations (arrowheads) are present between BDA labeled boutons and the labeled dendrites. A second lower magnification, higher magnification pair is shown in E and F. Scale in F = B–D.

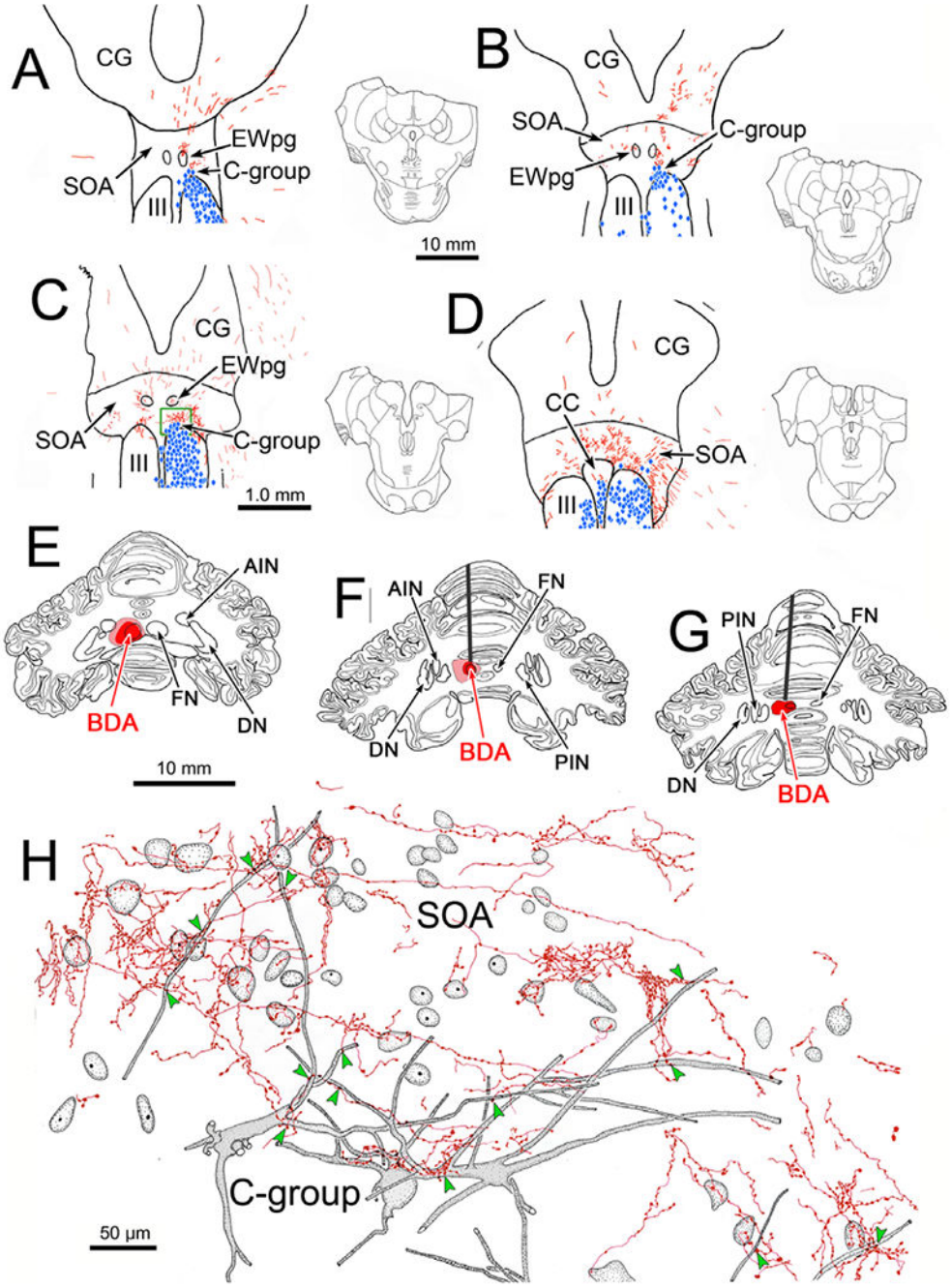

Fig. 6.

Distribution and morphology of BDA labeled fastigial terminals in the SOA. The BDA injection in this case was largely confined to the left fastigial nucleus (FN) (E–G). BDA labeled axons (red) terminated bilaterally, with a contralateral predominance, in the SOA (A–D). Injections of retrograde tracer into the extraocular muscles labeled motoneurons (blue diamonds) in the oculomotor nucleus (III) (A–D) and the C-group (A–C), and into the right levator muscle labeled motoneurons in the caudal central subdivision (CC) (D). Overlap between the distributions of labeled cells and terminals was present in the SOA

(A–D) and CC (F). Green box in C indicates area illustrated in H, where the relationship of fastigial boutons to C-group motoneurons is shown. Anterogradely labeled terminal arbors (red) overlap with the somata and dendrites of retrogradely labeled (gray shading) C-group motoneurons. Examples of close associations with boutons indicated by green arrowheads.

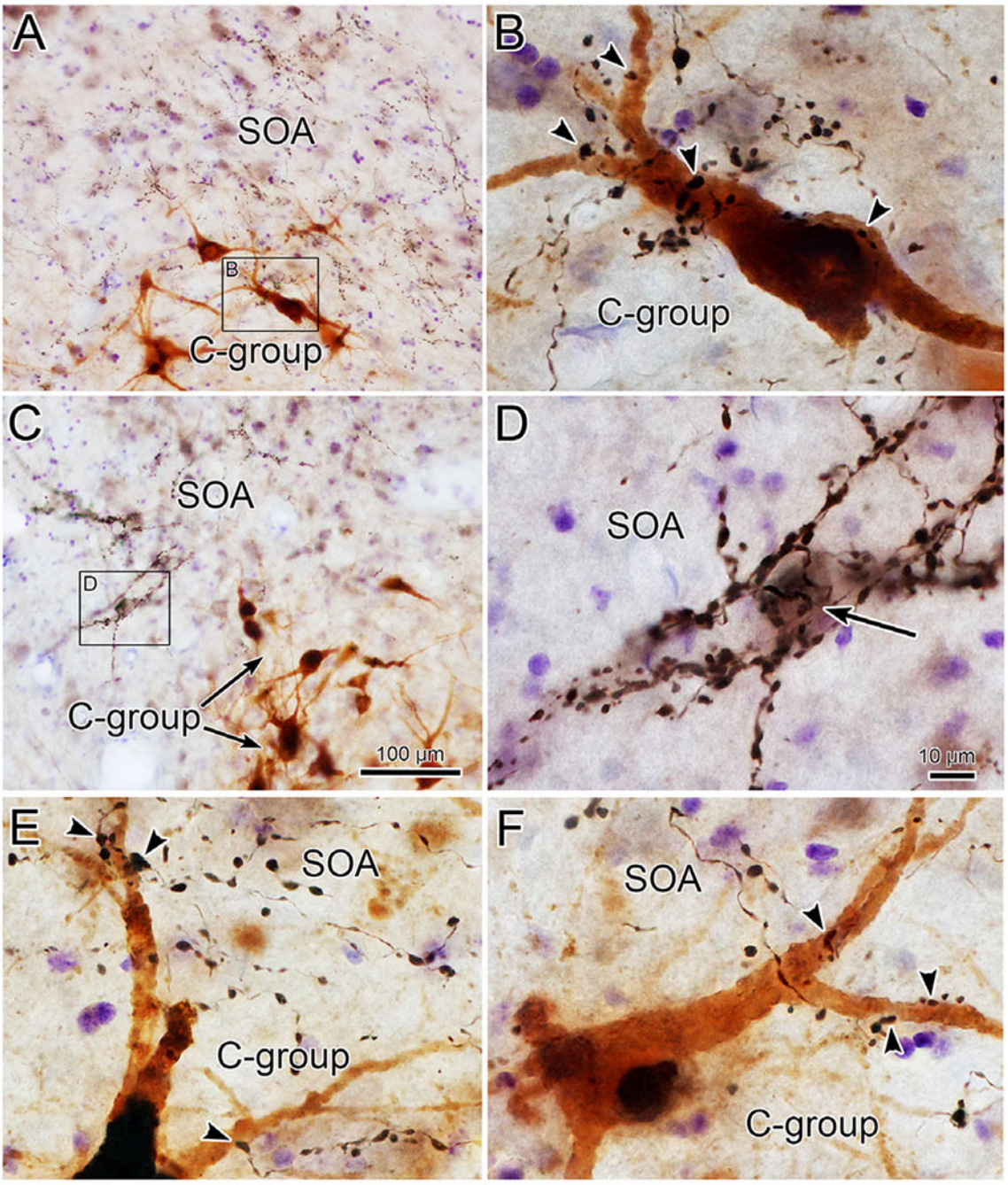

Fig. 7.

Close associations between fastigial boutons and C-group motoneurons (case illustrated in Fig. 6). The boxed region in A is shown at higher magnification in B. Close associations (arrowheads) are present between black, BDA labeled boutons and the brown, retrogradely labeled C-group motoneuron. Additional examples are shown in E and F. The fastigial terminal fields in SOA are better demonstrated in C, where the boxed region is presented at higher magnification in D. The counterstained cell (arrow) is surrounded by large numbers of BDA labeled boutons. Scale in C = A; in D = B, F, and E.

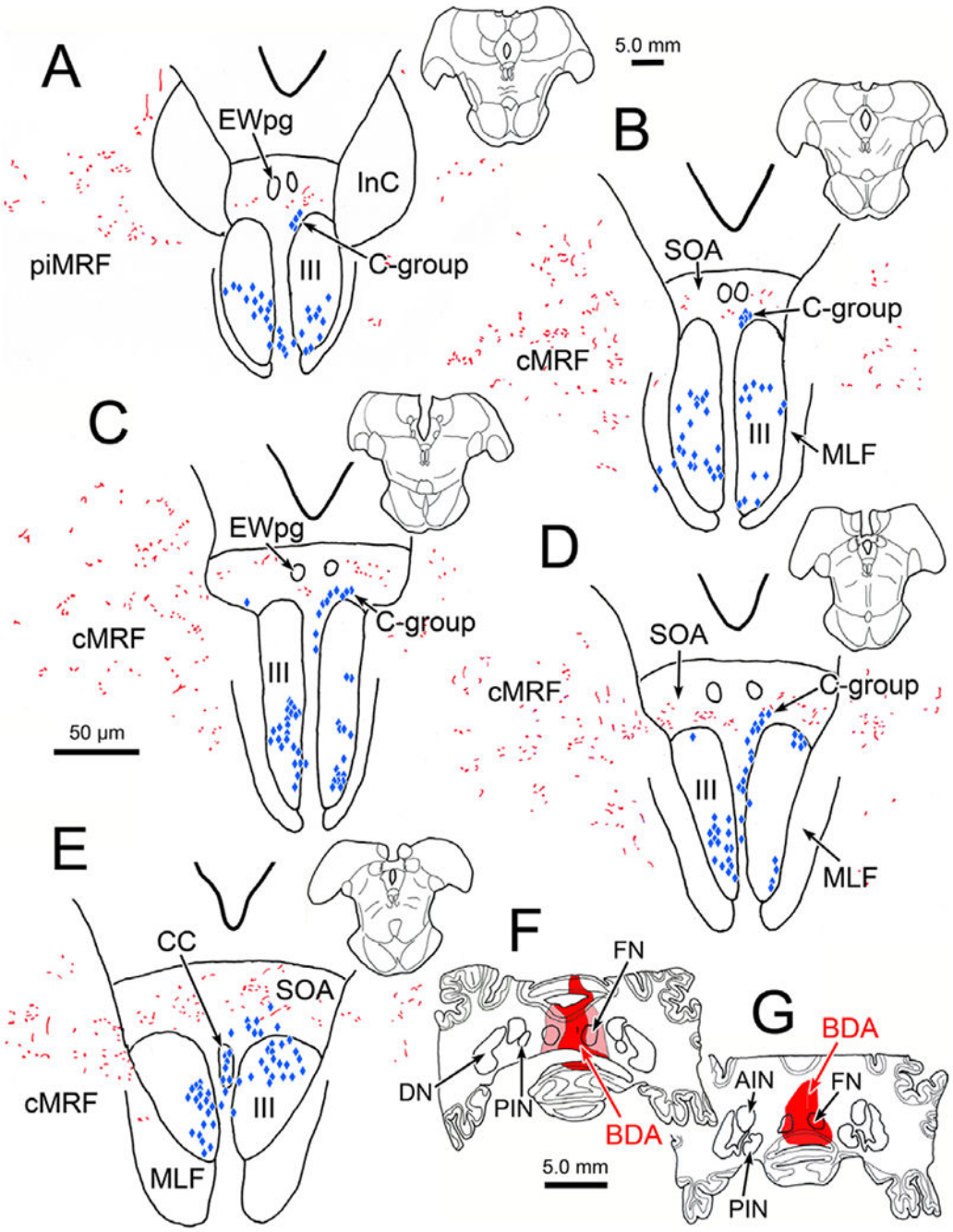

Fig. 8.

Distribution of fastigial terminal fields in the cMRF. The injection site involving both fastigial nuclei is shown in F and G. Anterogradely labeled terminals (red) are scattered through the cMRF on both sides (B–E). Retrogradely labeled superior rectus motoneurons are found in III, on the left, and medial rectus motoneurons are found in III on the right (blue diamonds).

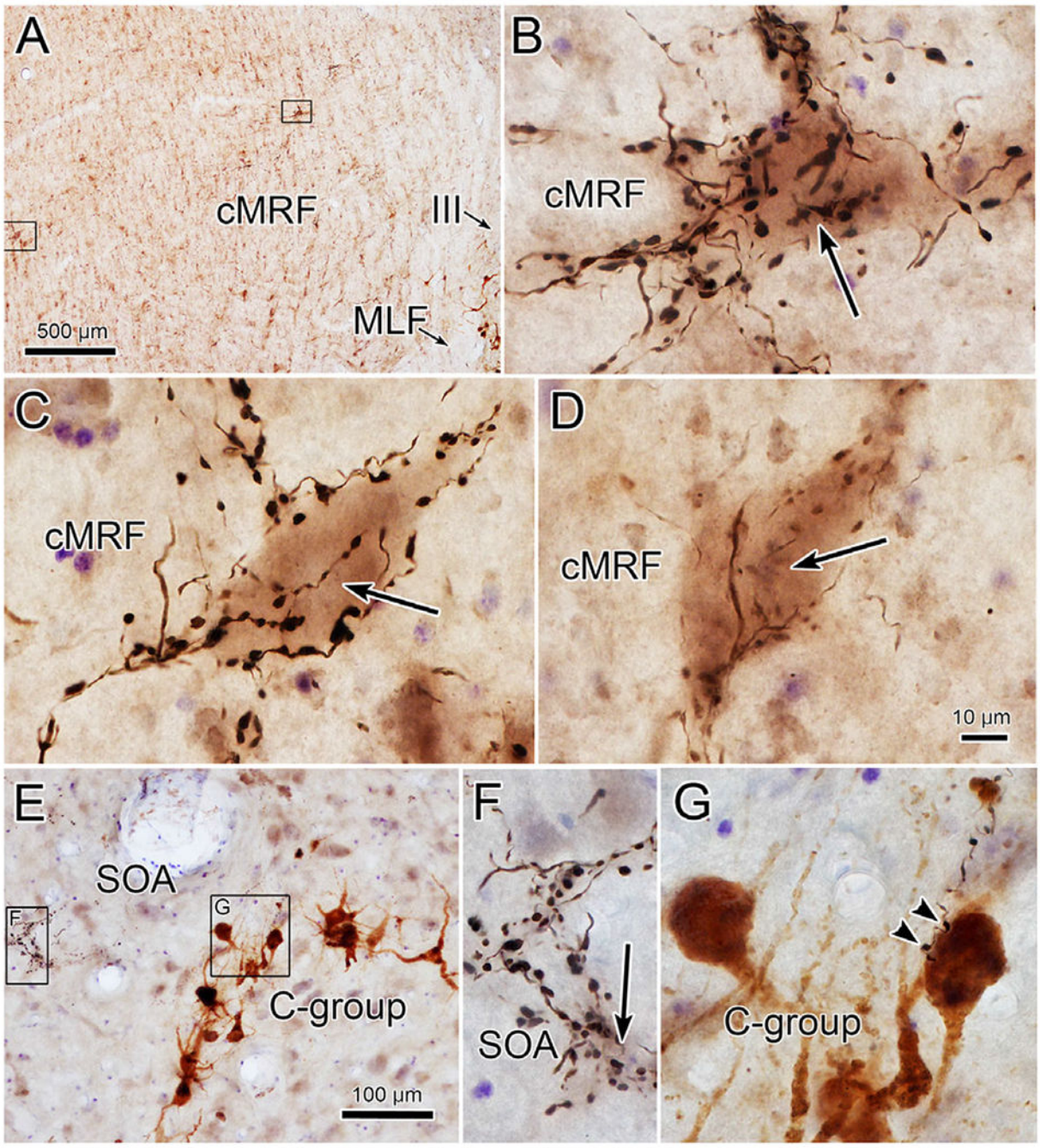

Fig. 9.

Fastigial boutons target a subpopulation of cells in the cMRF (from case illustrated in Fig. 8). The location of two intensively innervated neurons in the left cMRF is shown in A (left box—C, right box—B). High magnification views in B and C show how boutons enclose somata and proximal dendrites of the counterstained neuron (arrow). D shows an example from the right cMRF. Very few close associations (arrowheads) with C-group motoneurons, like that shown in G, were present in this case, but neurons intensely targeted by fastigial

boutons were present in the SOA (F). (In E, left box—F and right box—G). Scale D = B and C and F and G.

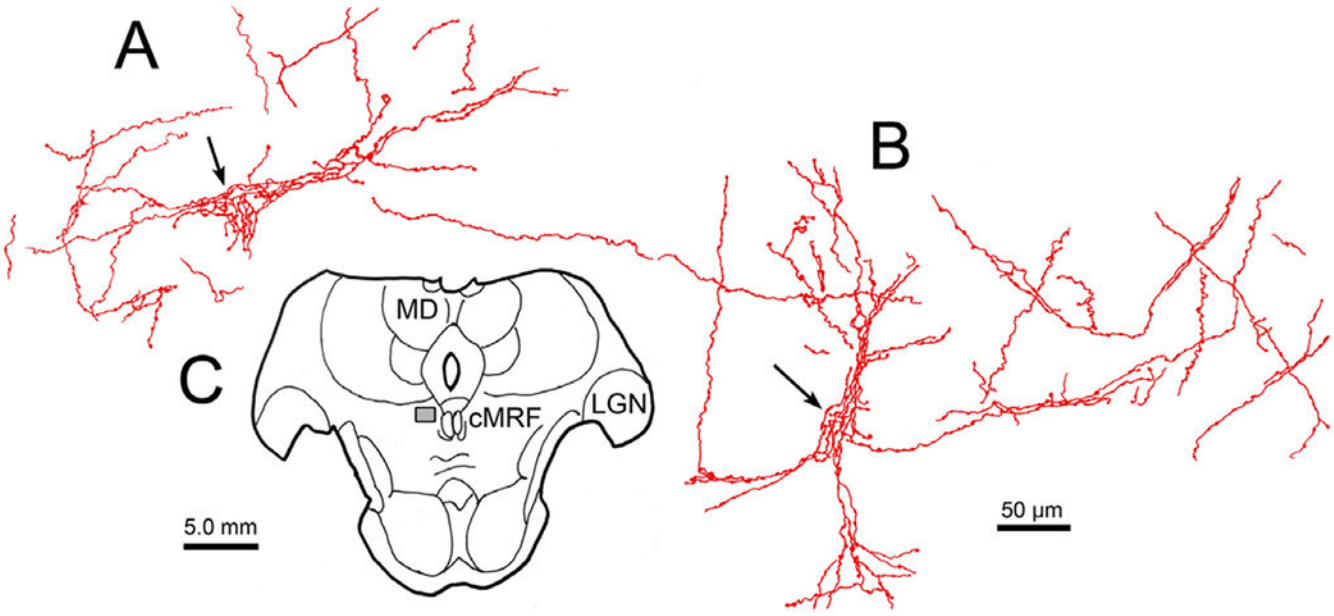

Fig. 10.

Fastigial boutons reveal dendritic fields of cMRF neurons. (A and B) Fastigial axons (red) with en passant boutons appear to extend out onto the dendrites of two examples of neurons in the cMRF. (C) Section showing region of the cMRF (box) where cells were located (same case as illustrated in Fig. 8).

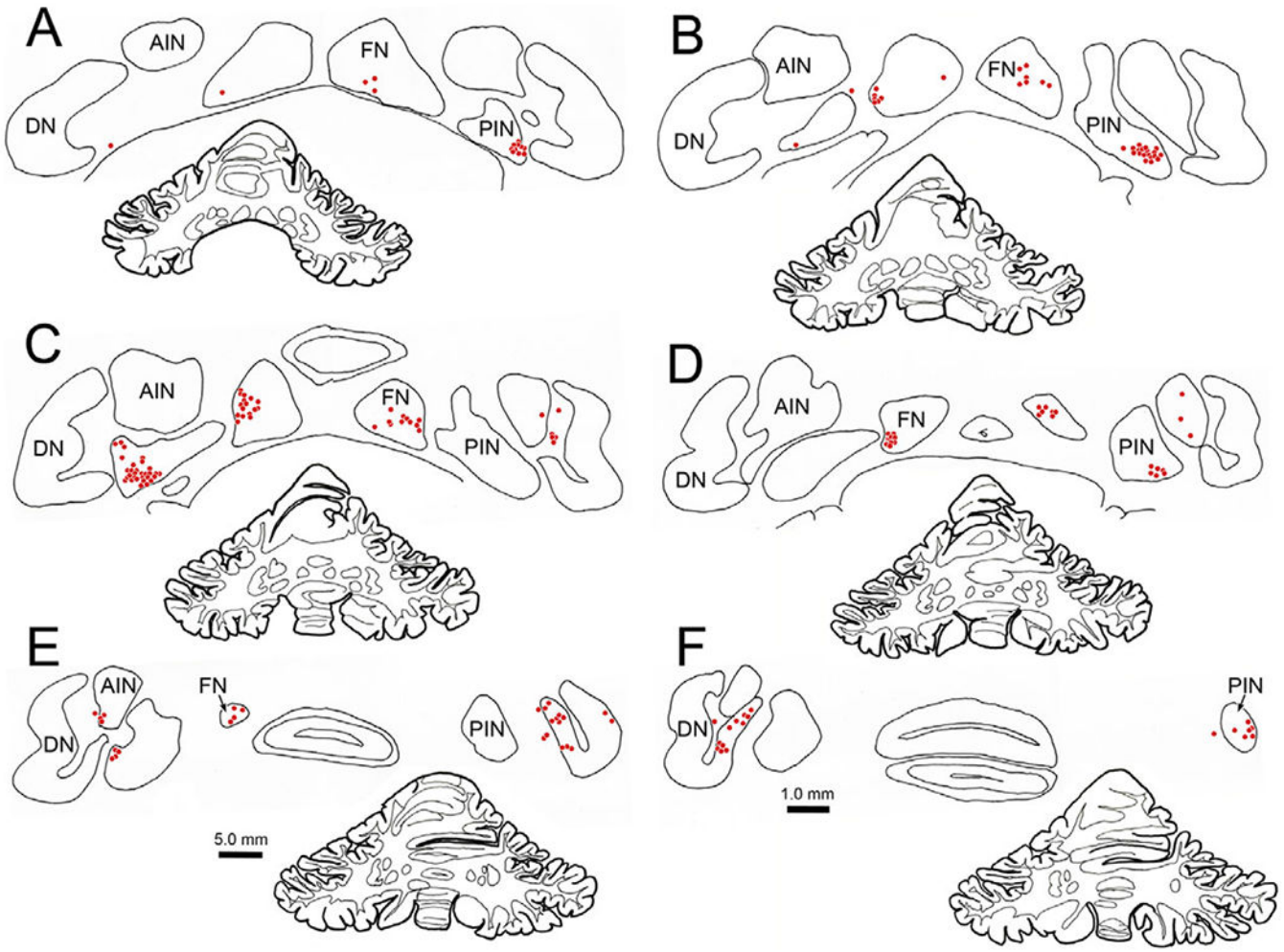

Fig. 11.

Distribution of lens accommodation-related neurons in the deep cerebellar nuclei. Following an injection of rabies N2c virus into the ciliary muscle of the left eye, trans-synaptic retrograde transport labels cells (red dots) bilaterally in the deep cerebellar nuclei following an 84 h survival. Prominent populations of cells were located in the fastigial nucleus (FN) (A–E) and posterior interposed nucleus (PIN) (A–F). A smaller population was found in the dentate nucleus (DN) (E and F).

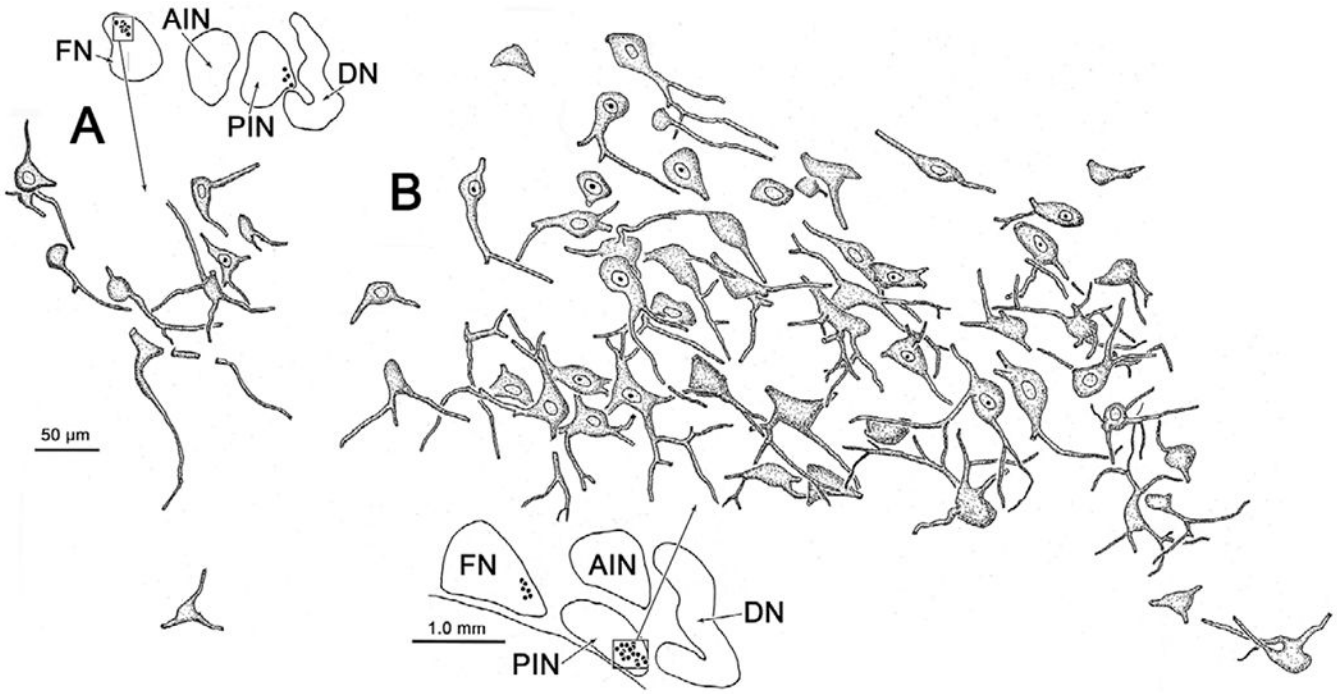

Fig. 12.

Morphology of the lens accommodation-related neurons in the deep cerebellar nuclei. Relatively small, multipolar neurons located in the fastigial nucleus (FN) (A) and posterior interposed nucleus (PIN) (B) were labeled with the rabies virus in the case illustrated in Fig. 11. The labeled cells generally formed a tight cluster. Low magnification inserts show the area (box) containing the illustrated labeled cells (dots).

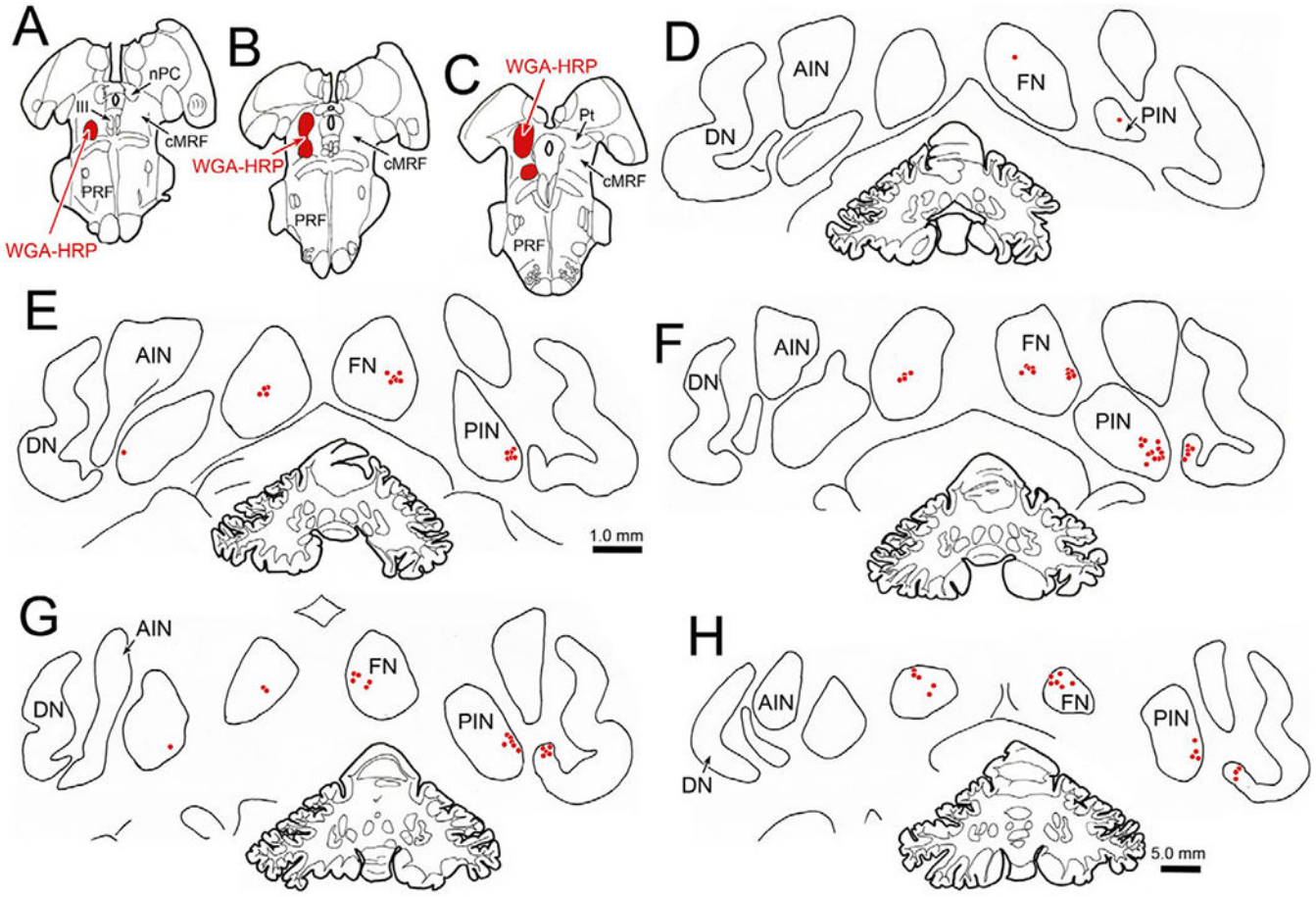

Fig. 13.

Distribution of cerebellar neurons supplying input to the cMRF. An injection of WGA-HRP into the cMRF (A–C) produced retrogradely labeled neurons (red dots) in the deep cerebellar nuclei (D–H). Labeled neurons were observed bilaterally in the fastigial nucleus (FN) (D–H) and contralaterally in the posterior interposed nucleus (PIN) (D–H) and adjacent dentate nucleus (DN) (F–H).